Optical Interferometry

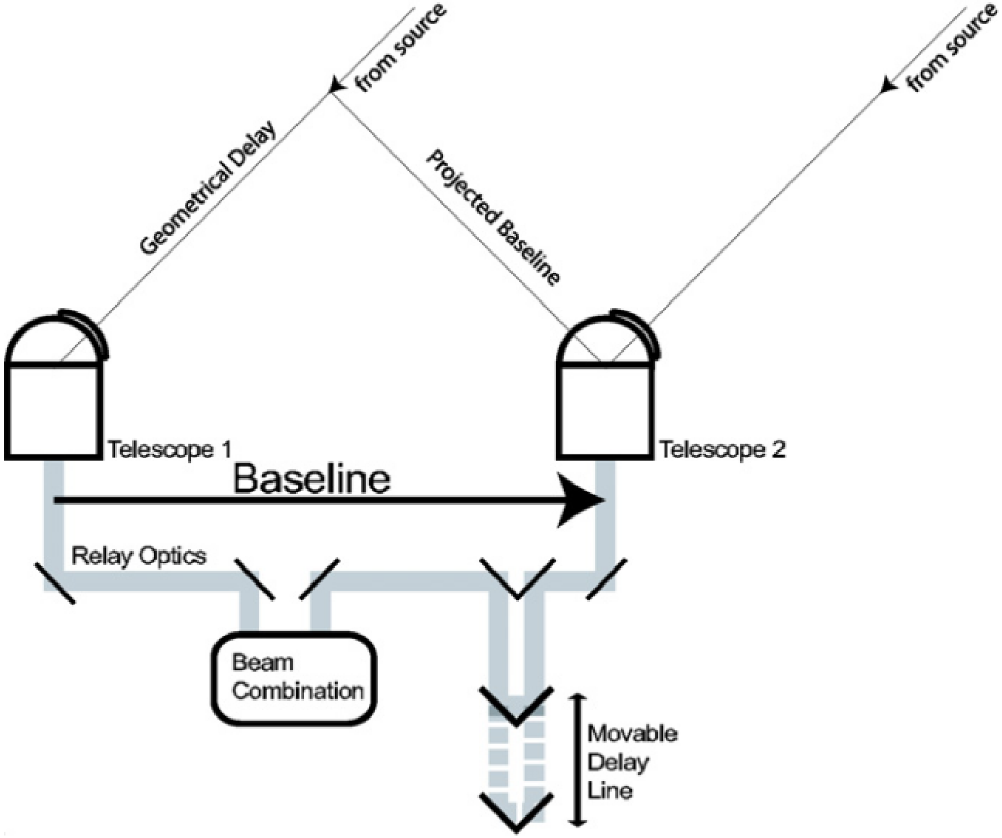

CV

- ESO Fellowship – 2022 - present
  - 50% independent science
  - 50% observatory duties including 80 observing nights/year at the VLT
- Postdoc at CHARA (2017-2022)
  - 70% independent science
  - 30% observatory duties – observing nights, visitor support, work in optical lab

- PhD in Prague with 1-year ESO Studentship (2012-2017)
  - Modeling of Be star disks with Stanislav Štefl Daniela Korčáková
- Mgr. in Brno with 4-month ESO internship (2010-2012)
  - Disentangling of spectra & light curve analysis of eclipsing binaries with Petr Hadrava
- Bc. in Brno (2007-2010)
  - UV spectroscopy of central stars of planetary nebulae with Jiří Krtička

robertklement@gmail.com

Optical Interferometry

- Lecture 1
  - Basic principles and History
  - Atmospheric turbulence and how to overcome it
  - Subsystems of an interferometric observatory – CHARA and VLTI
  - Interferometric observables
- Lecture 2
  - Visualizing interferometric data & basic interpretation
  - Planning observations
  - JMMC tools for interferometry (https://www.jmmc.fr/)
- Lecture 3
  - Parametric fitting of interferometric data with PMOIRED (https://github.com/amerand/PMOIRED)

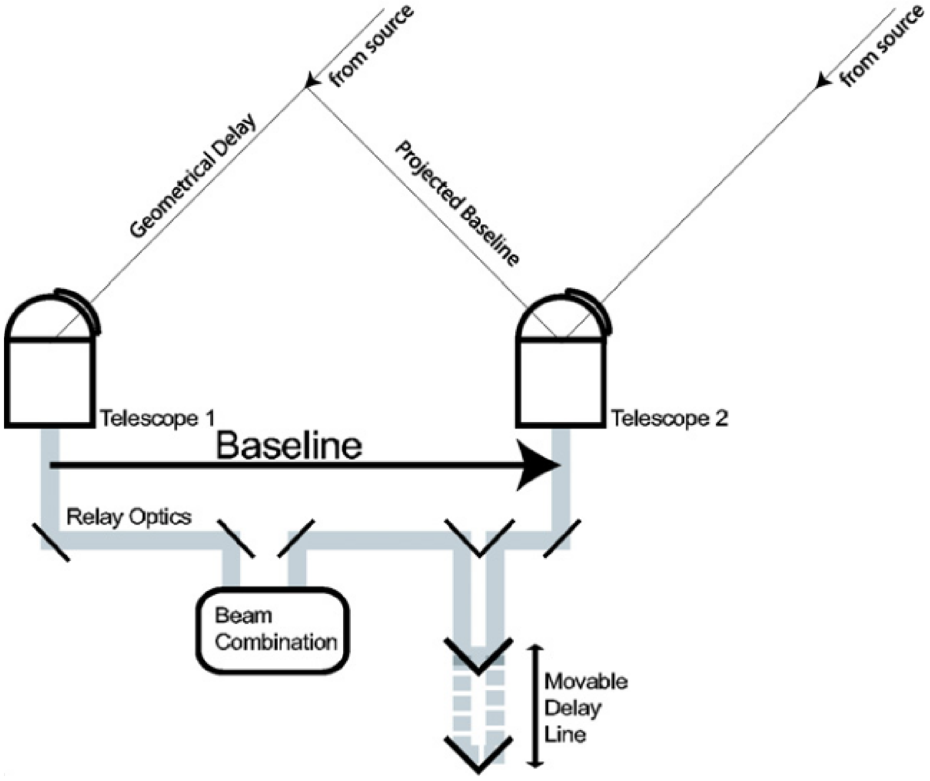

Intro - Resources

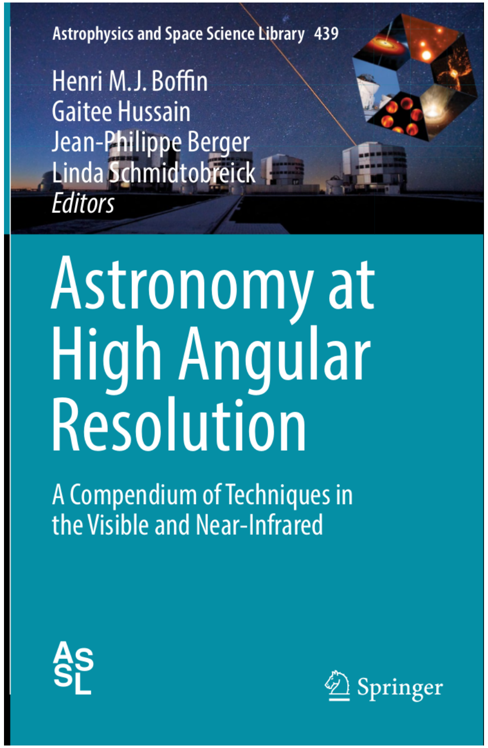

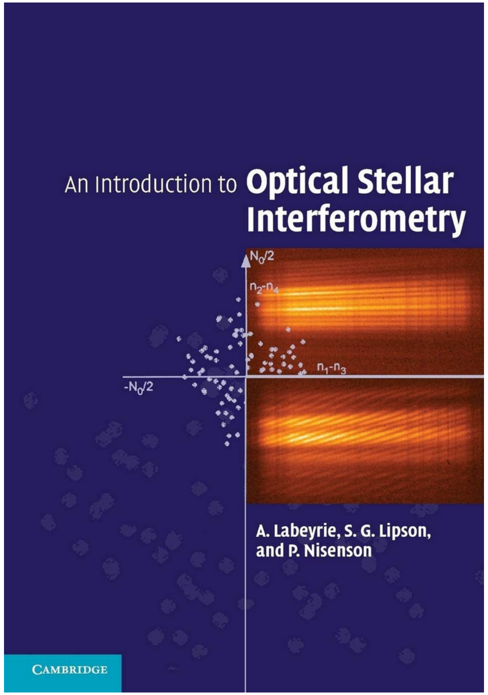

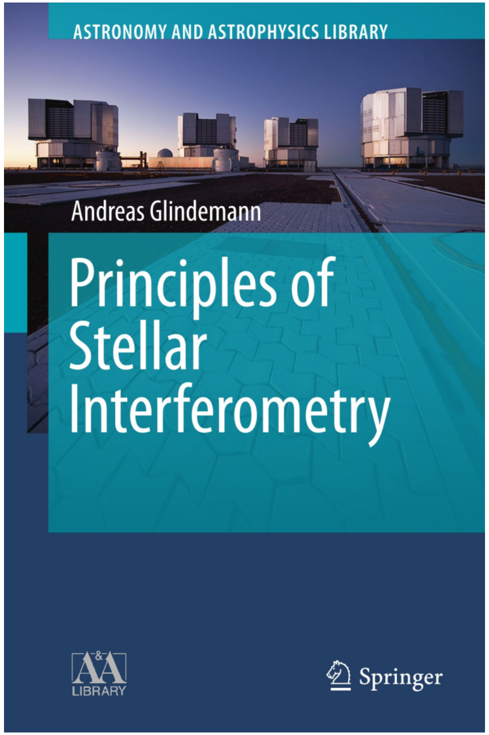

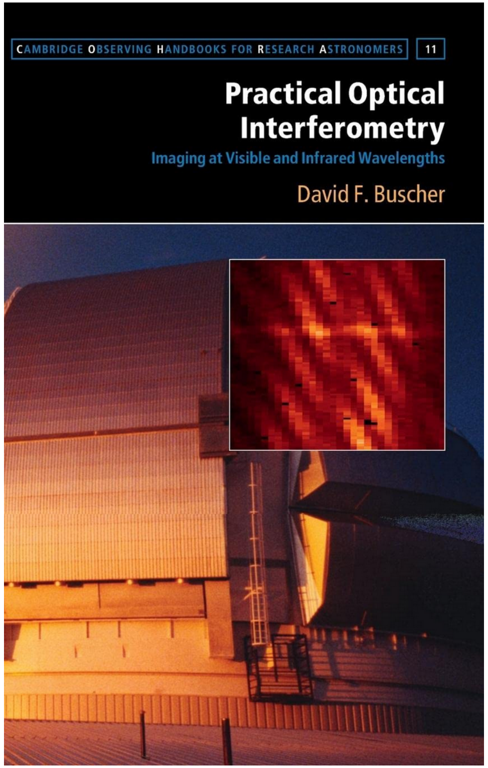

Annual Review of Astronomy and Astrophysics

Advances in Optical/Infrared Interferometry

Frank Eisenhauer,[1] John D. Monnier,[2] and Oliver Pfuhl[3]

[1]Max Planck Institute for Extraterrestrial Physics, Garching, Germany; email: eisenhau@mpe.mpg.de

[2]Astronomy Department, University of Michigan, Ann Arbor, Michigan, USA; email: monnier@umich.edu

[3]European Southern Observatory, Garching, Germany; email: opfuhl@eso.org

Annu. Rev. Astron. Astrophys. 2023. 61:237–85

First published as a Review in Advance on June 7, 2023

The *Annual Review of Astronomy and Astrophysics* is online at astro.annualreviews.org

https://doi.org/10.1146/annurev-astro-121622-045019

Keywords

instrumentation, Galactic Center, exoplanets, active galactic nuclei, young stellar objects, stars

Abstract

After decades of fast-paced technical advances, optical/infrared (O/IR) interferometry has seen a revolution in recent years:

- The GRAVITY instrument at the Very Large Telescope Interferometer (VLTI) with four 8-m telescopes reaches thousand-times-fainter objects than possible with earlier interferometers, and the Center for High Angular Resolution Astronomy array (CHARA) routinely offers up to 330-m baselines and aperture synthesis with six 1-m telescopes.
- The observed objects are fainter than 19 mag, the images have sub-milliarcsecond resolution, and the astrometry reaches microarcsecond precision.
- This led to breakthrough results on the Galactic Center, exoplanets, active galactic nuclei, young stellar objects, and stellar physics.

Following a primer in interferometry, we summarize the advances that led to the performance boost of modern interferometers:

- Single-mode beam combiners now combine up to six telescopes, and image reconstruction software has advanced over earlier developments for radio interferometry.
- With a combination of large telescopes, adaptive optics (AO), fringe tracking, and especially dual-beam interferometry, GRAVITY has boosted the sensitivity by many orders of magnitude.

Diffraction limit of a single telescope

$$\Delta\theta = 1.22\,\lambda / D$$

- Bigger telescope (large *D*) gives better angular resolution (small *Δθ*)
- Atmospheric seeing limits angular resolution for *D* > 20 cm (for r_0 = 20 cm)
- Reaching the diffraction limit on single-dish telescopes: AO and other
- Beyond what is possible with large telescopes: interferometry

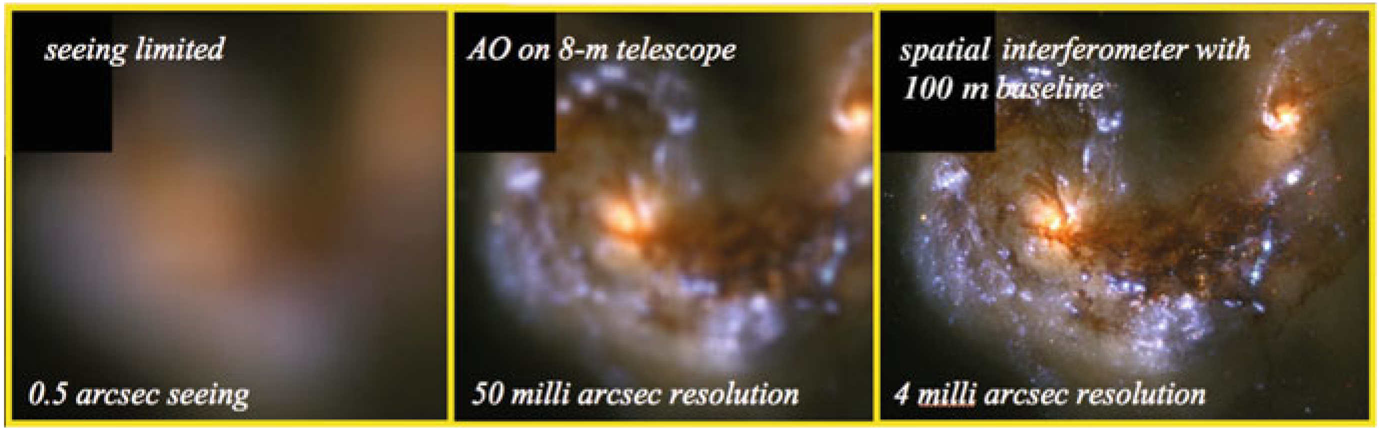

Diffraction limit of a single telescope

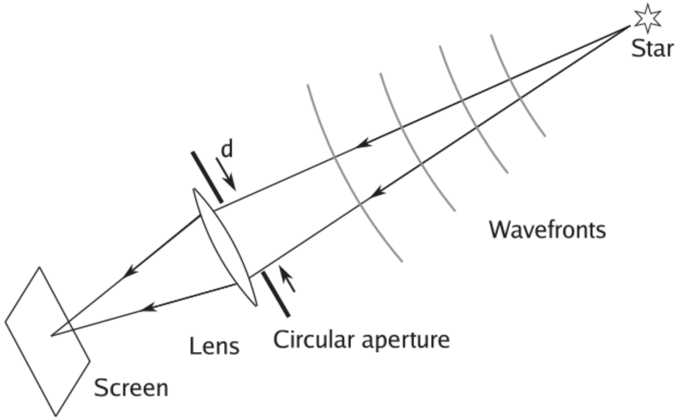

$$\Delta\theta = 1.22\,\lambda/D$$

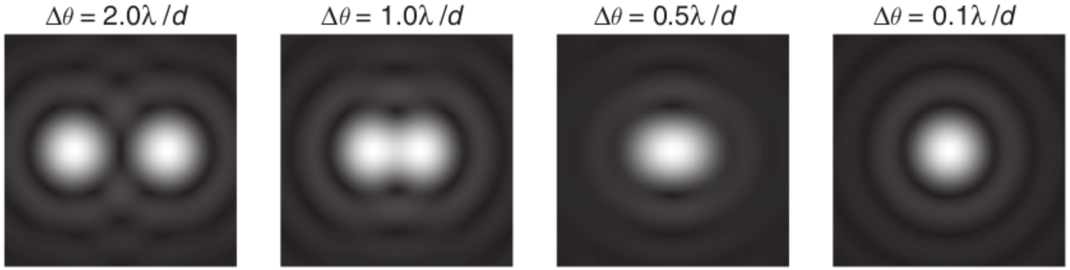

- **Airy disk** – ideal diffraction-limited image of a point source
- **Point spread function (PSF)** – through an actual telescope (and atmosphere)
- Observed image is a convolution of the ideal image function with the PSF

Impact of atmosphere on observations

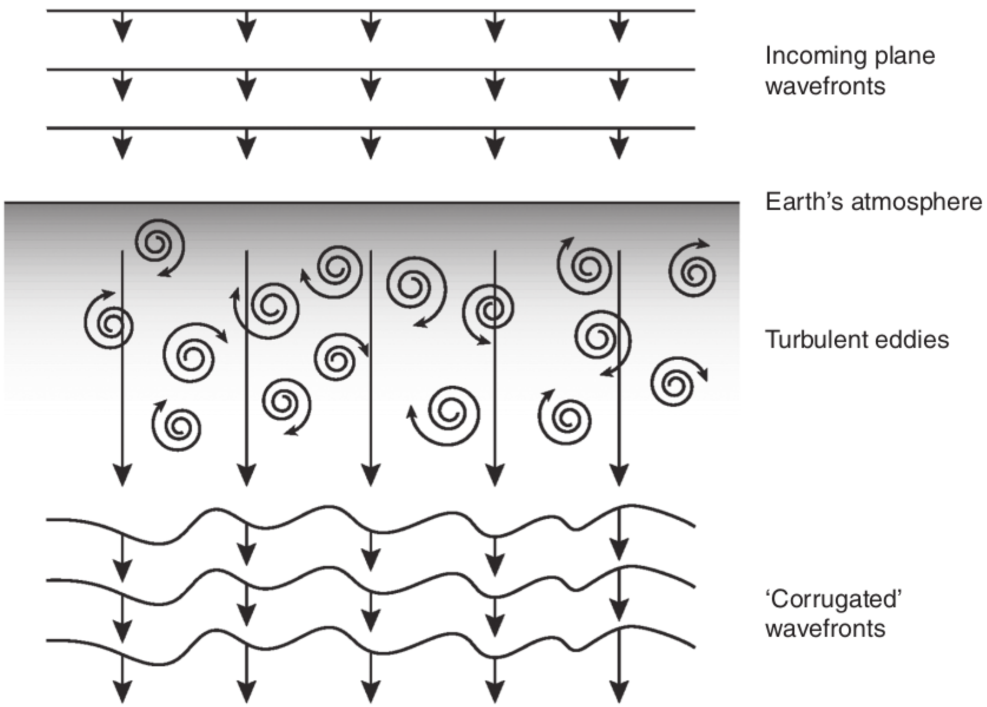

Impact of atmosphere on observations

The **Fried parameter *r_0*** - diameter of a circular patch of the incoming wavefront with phase variance of ~1 rad^2

$$r_0 = \left(0.423\left(\frac{2\pi}{\lambda}\right)^2 (\cos\zeta)^{-1}\int C_n^2(h)\mathrm{d}h\right)^{-3/5}$$

$$r_0 \propto \lambda^{6/5} \qquad r_0 \propto \cos(\zeta)^{3/5}$$

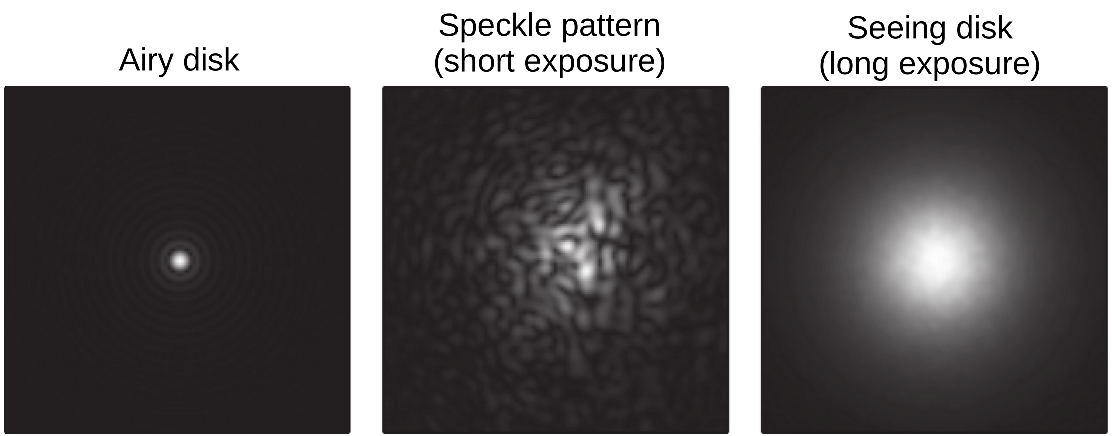

Atmospheric **coherence time** is the time difference when the rms phase fluctuations at a single point have a value of 1 rad

$$\tau_0 = 0.314\,\frac{r_0}{\bar{v}} = \left(2.91\left(\frac{2\pi}{\lambda}\right)^2 \int C_n^2(h)v^{5/3}\mathrm{d}h\right)^{-3/5}$$

$$FWHM_{seeing} = 0.98\,\lambda / r_0$$

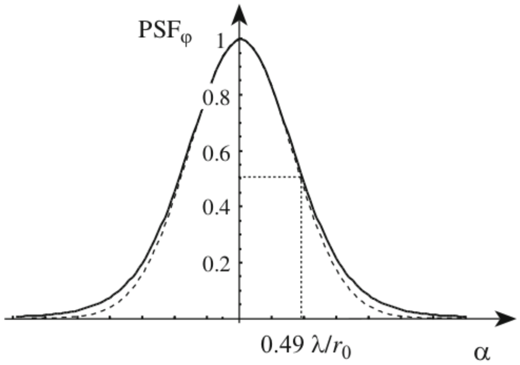

Reaching diffraction limit

- The fight against atmosphere on single telescopes
  - **Aperture masking**
  - Lucky/speckle imaging / speckle interferometry
  - AO-assisted Imaging

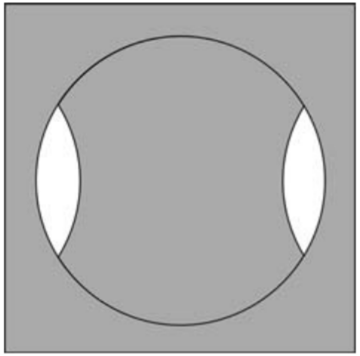

Aperture mask used by Stephan on 80-cm reflector

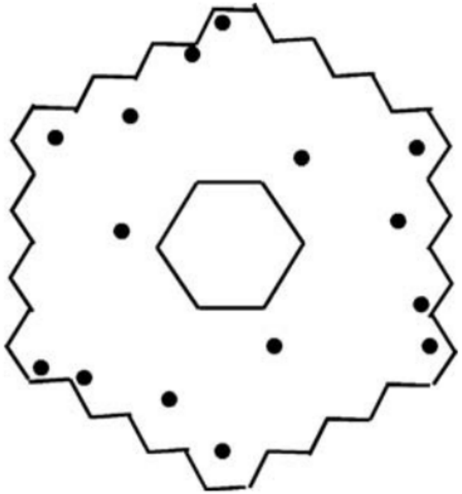

Nonredundant aperture mask on the 10-m Keck multimirror telescope.

Reaching diffraction limit

- The fight against atmosphere on single telescopes
  - Aperture masking
  - **Lucky/speckle imaging / speckle interferometry**
  - AO-assisted Imaging

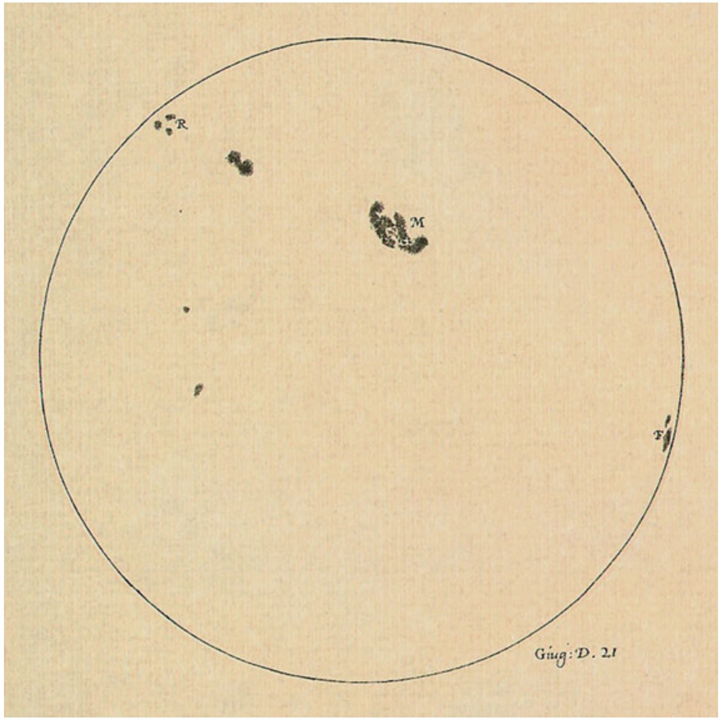

The Sun on 21 June 1613 as recorded by Galileo Galilei

Reaching diffraction limit

- The fight against atmosphere on single telescopes
  - Aperture masking
  - Lucky/speckle imaging / speckle interferometry
  - **Adaptive Optics**

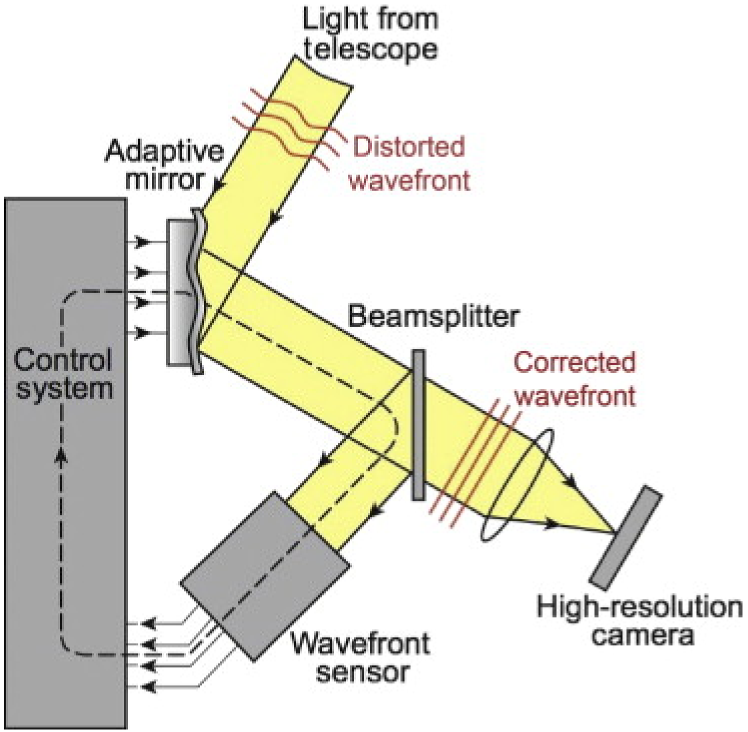

AO concept

Interferometry

$$\Delta\theta = 1.22\,\lambda/2\,B$$

Variation on Young’s double-slit experiment - incoming light passes through two apertures and forms interference pattern

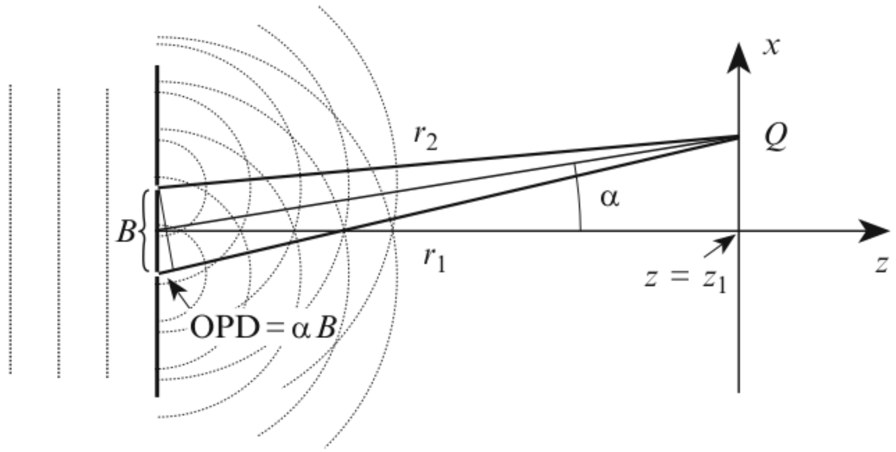

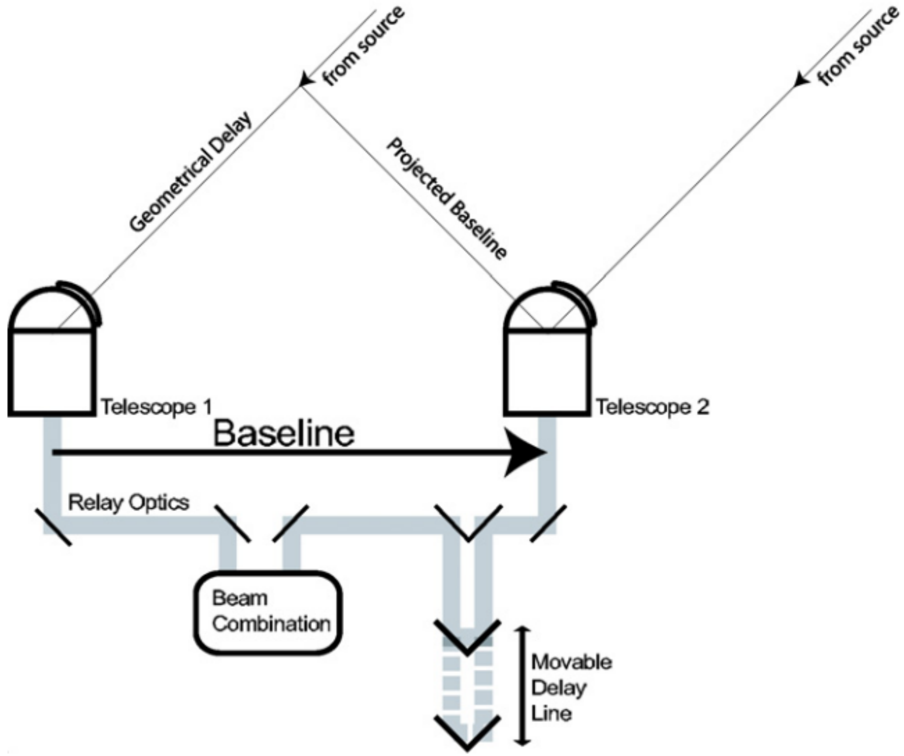

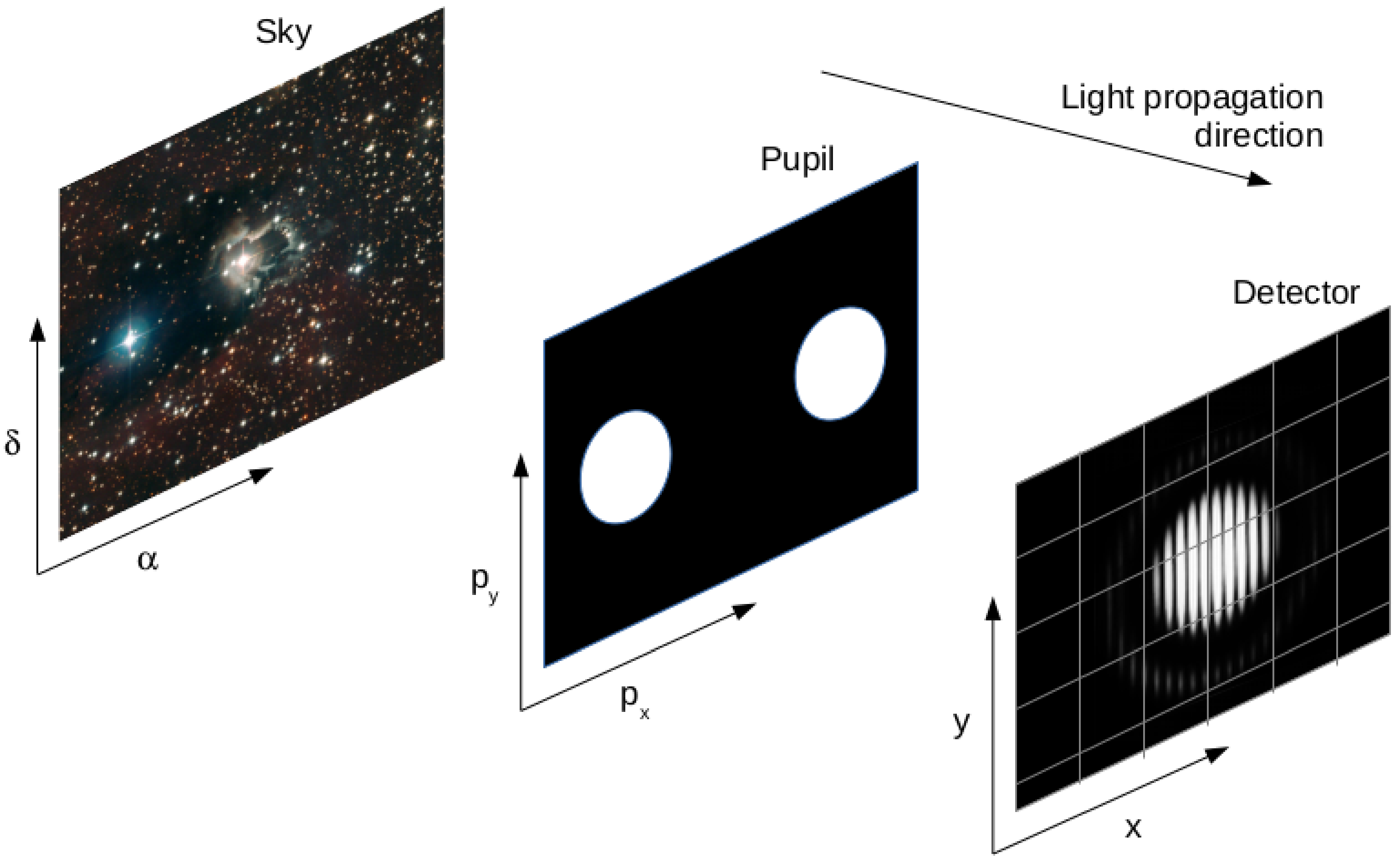
Sky
δ
α
Light propagation
direction
Pupil
p_y
p_x
Detector
y
x

History

- 1868 – Fizeau – aperture masking – demonstrated in 1874 by Stéphan
- 1890 – Michelson (1891) measures the size of the moons of Jupiter
- **1921 – Michelson & Pease measure the size of Betelgeuse (47 mas) using 20-ft beam**
- 1931 – Pease measures another six stars using 20-ft beam and one star using 50-ft beam
- 1940s – First applied to radio astronomy
- 1950s – Aperture synthesis with movable antennas
- 1956 – Intensity interferometry (Hanbury Brown & Twiss 1956)
- 1960s-1970s – Aperture synthesis by Earth's rotation (VLA), also VLBI
- 1970 – Speckle interferometry (Labeyrie 1970)
- **1974 – First coherent combination using two separate telescopes (Labeyrie 1975)**
- 1980s-1990s – GI2T, Mark I-III (first active fringe tracking), PTI (first dual-feed system), IOTA, COAST (first closure phase image), NPOI, SUSI, ISI (mid-IR)
- 2000s – Keck Interferometer, VLTI, CHARA
- **2010s – AO & 2nd generation instruments at VLTI (GRAVITY) and CHARA**
- 2020-2030s – MROI, Michelson CHARA Array, GRAVITY+

History

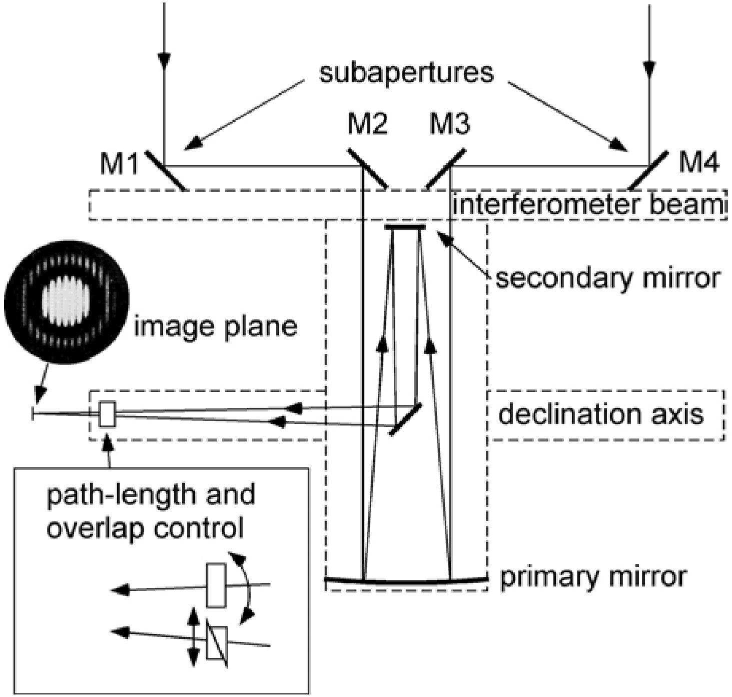

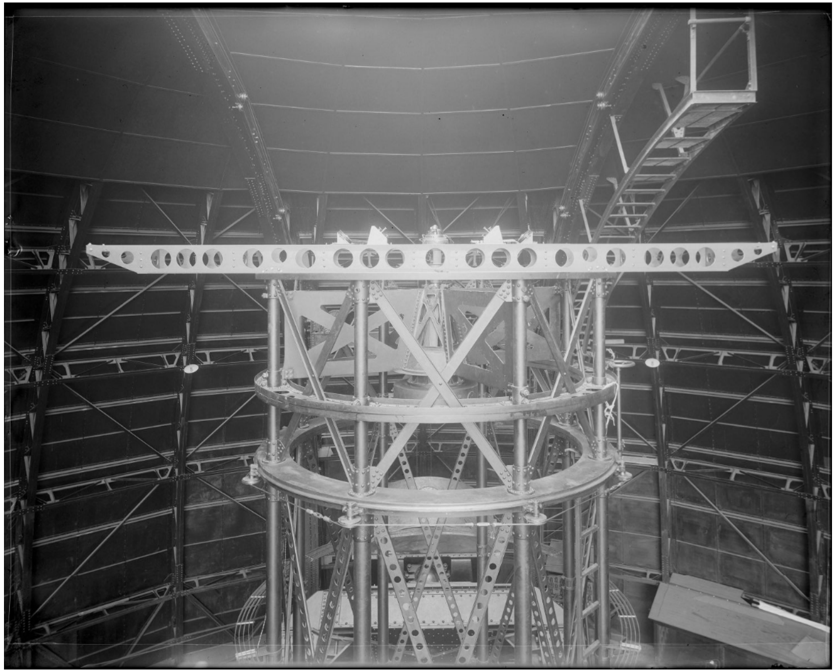

Michelson's 20-foot beam stellar interferometer. (a) Optical diagram; (b) a photograph of the instrument, as it is today in the Mount Wilson Museum (reproduced by permission of the Huntington Library).

History

- 1868 – Fizeau – aperture masking – demonstrated in 1874 by Stéphan
- 1890 – Michelson (1891) measures the size of the moons of Jupiter
- **1921 – Michelson & Pease measure the size of Betelgeuse (47 mas) using 20-ft beam**
- 1931 – Pease measures another six stars using 20-ft beam and one star using 50-ft beam
- 1940s – First applied to radio astronomy
- 1950s – Aperture synthesis with movable antennas
- 1956 – Intensity interferometry (Hanbury Brown & Twiss 1956)
- 1960s-1970s – Aperture synthesis by Earth's rotation (VLA), also VLBI
- 1970 – Speckle interferometry (Labeyrie 1970)
- **1974 – First coherent combination using two separate telescopes (Labeyrie 1975)**
- 1980s-1990s – GI2T, Mark I-III (first active fringe tracking), PTI (first dual-feed system), IOTA, COAST (first closure phase image), NPOI, SUSI, ISI (mid-IR)
- 2000s – Keck Interferometer, VLTI, CHARA
- **2010s – AO & 2nd generation instruments at VLTI (GRAVITY) and CHARA**
- 2020-2030s – MROI, Michelson CHARA Array, GRAVITY+

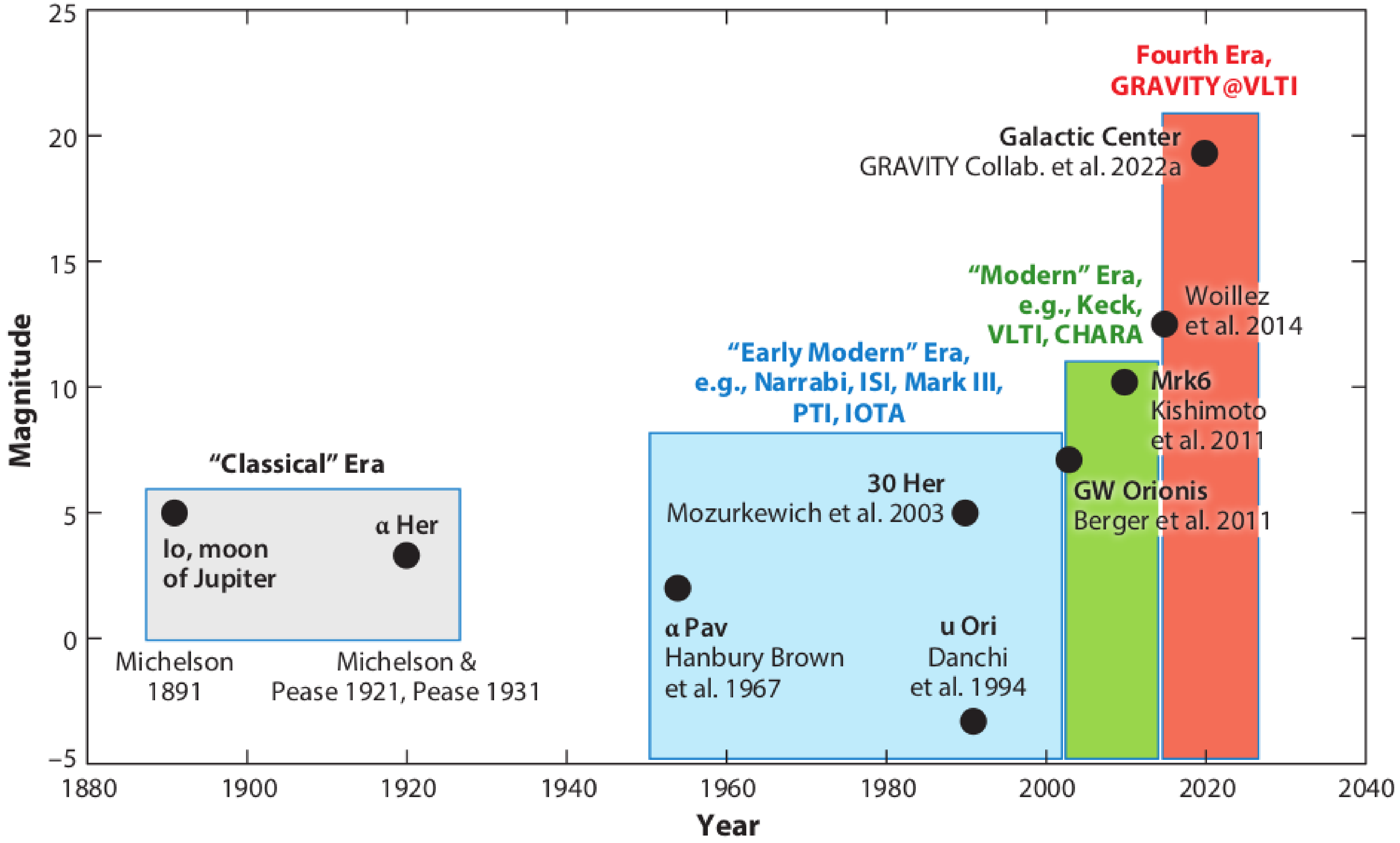
Fourth Era,
GRAVITY@VLTI
Galactic Center
GRAVITY Collab. et al. 2022a
"Modern" Era,
e.g., Keck,
VLTI, CHARA
Woillez
et al. 2014
"Early Modern" Era,
e.g., Narrabi, ISI, Mark III,
PTI, IOTA
Mrk6
Kishimoto
et al. 2011
"Classical" Era
30 Her
Mozurkewich et al. 2003
GW Orionis
Berger et al. 2011
α Her
Io, moon
of Jupiter
α Pav
Hanbury Brown
et al. 1967
u Ori
Danchi
et al. 1994
Michelson
1891
Michelson &
Pease 1921, Pease 1931
Magnitude
Year
25
20
15
10
5
0
−5
1880
1900
1920
1940
1960
1980
2000
2020
2040

Interferometry

CHARA

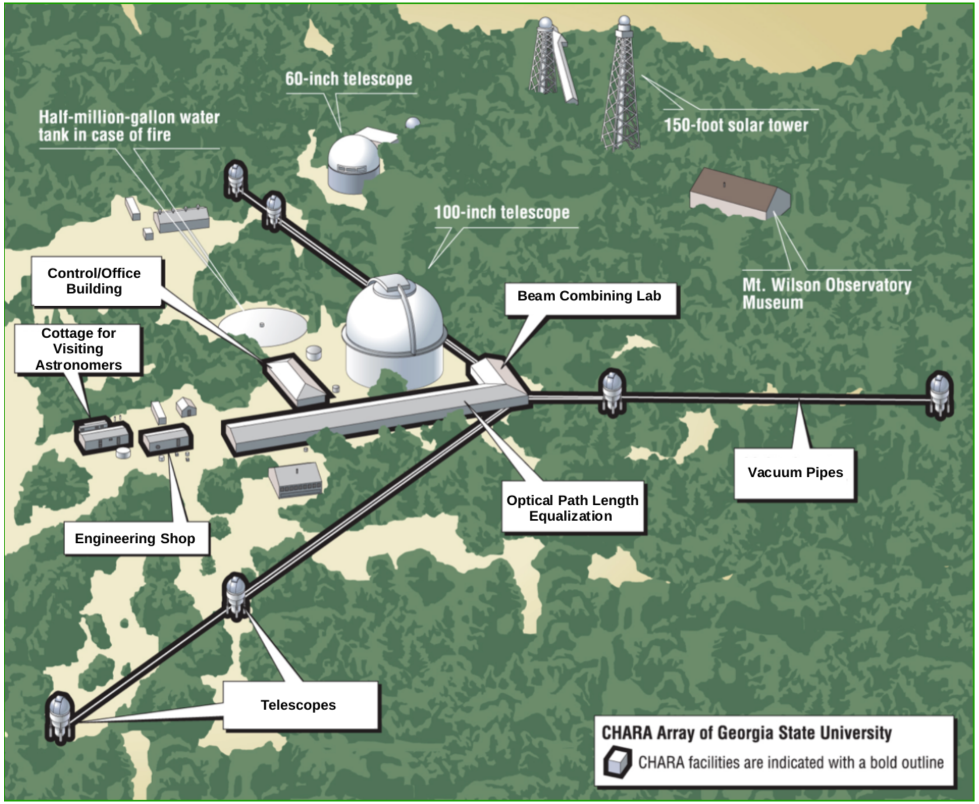

VLTI

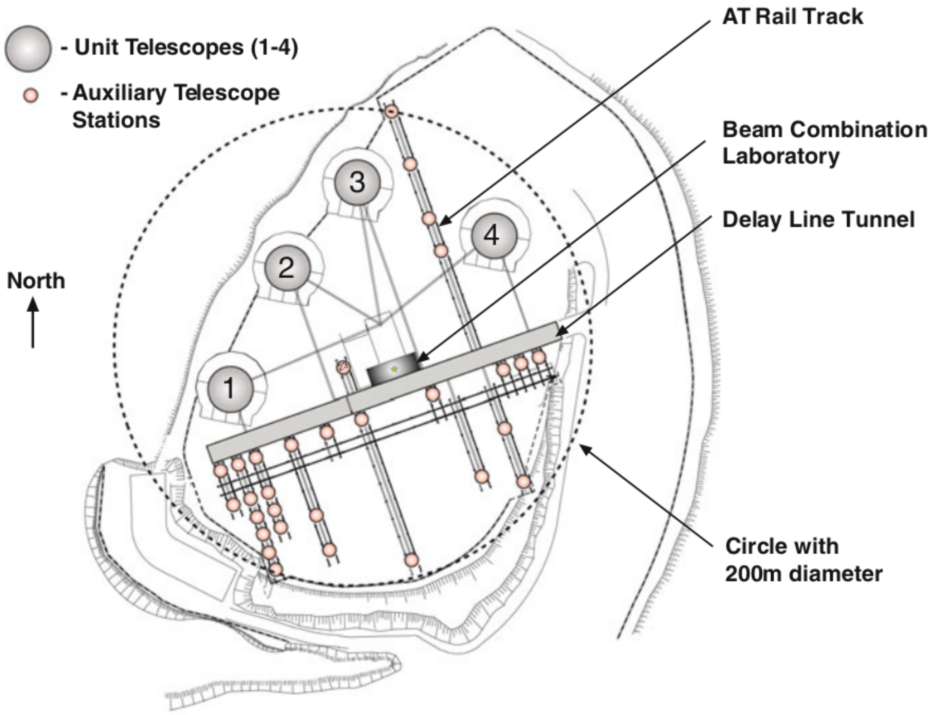

Radio interferometry

VLA

- 27 antennas (25m)
- 4 configurations
- λ = 0.6 – 30 cm
- θ ~ 40 mas

ALMA

- 66 reconfigurable antennas (12m and 7m)
- 192 possible antenna locations
- λ = 0.3 – 3 mm
- θ ~ 15 mas

Event Horizon Telescope

- $\lambda = 1.3$ mm
- $\theta \sim 10$ μas

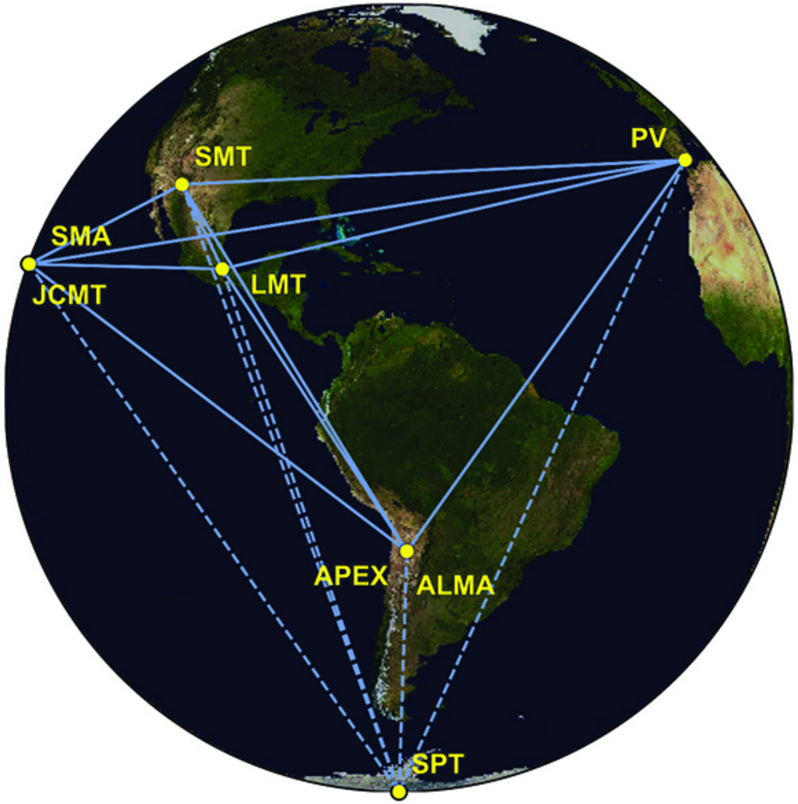

M87

Simple 2-telescope interferometer

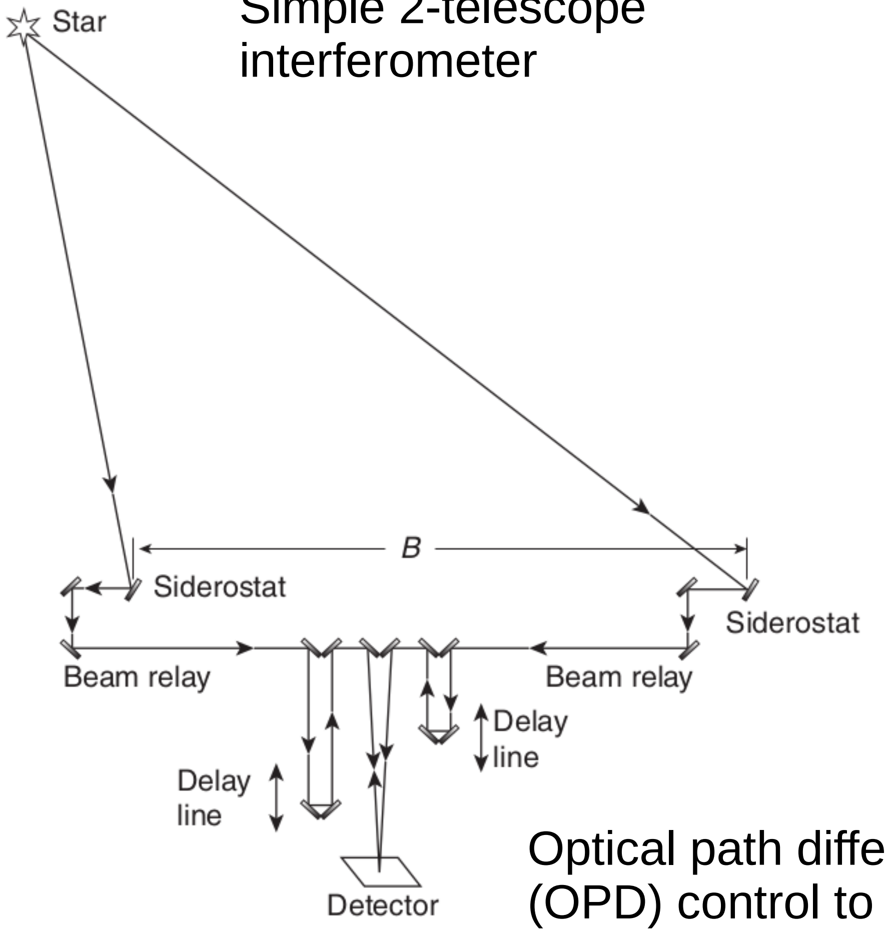

Optical path difference (OPD) control to enable coherent combination

Beam combination

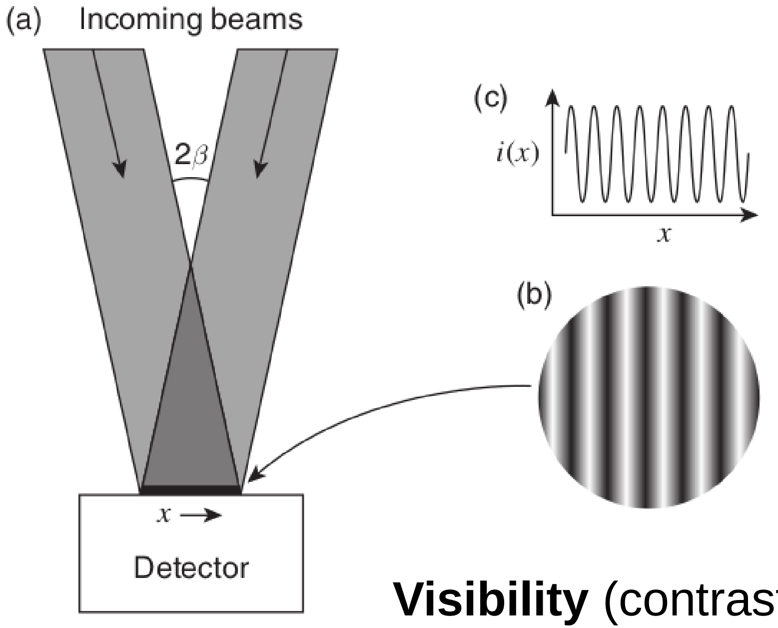

Visibility (contrast) and **Phase** (position) of interferometric fringes contain high angular resolution information on the observed object

(u,v)-plane

- Baselines of telescope pairs are given in the **(u,v)-plane - ** a plane in Fourier space where each point corresponds to a spatial frequency in the sky plane
- Measurement at each baseline *(u,v)* gives a **Fourier component of the sky brightness distribution** *(l,m)*
- **Aperture synthesis** – combining multiple baselines

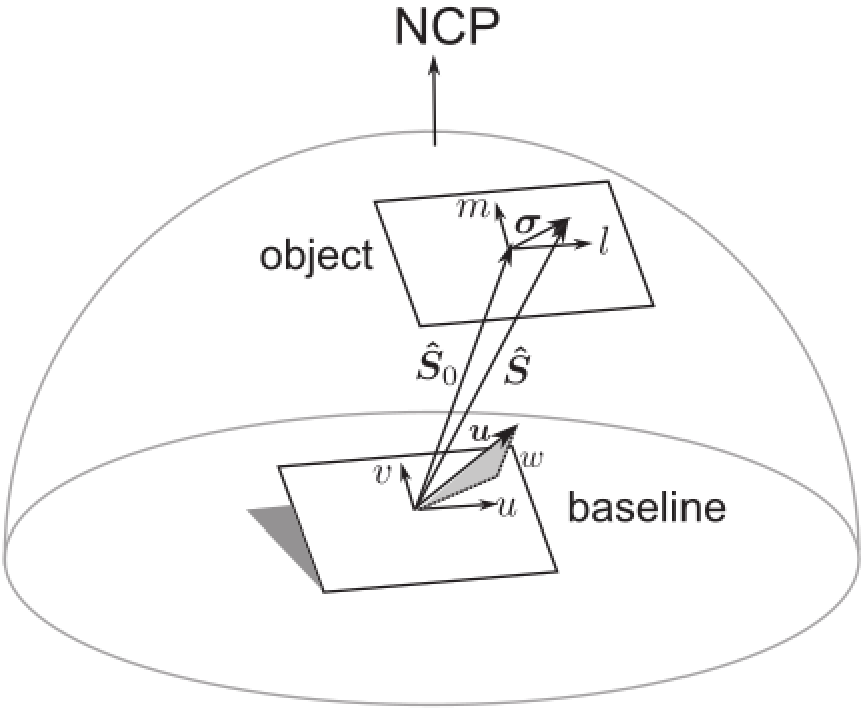

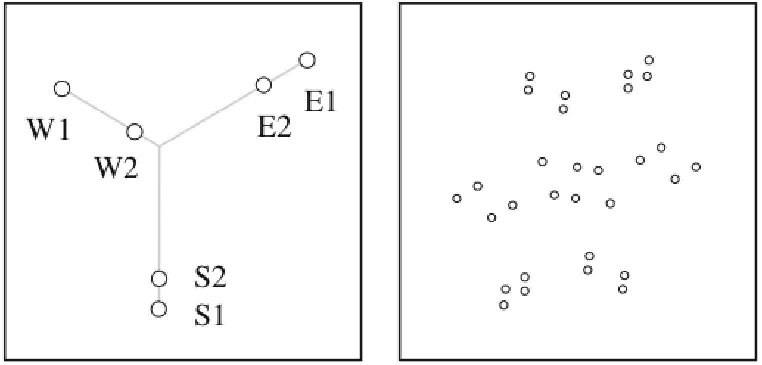

CHARA array uv-plane

(u,v)-plane

- Baselines of telescope pairs are given in the **(u,v)-plane - ** a plane in Fourier space where each point corresponds to a spatial frequency in the sky plane
- Measurement at each baseline *(u,v)* gives a **Fourier component of the sky brightness distribution** *(l,m)*
- **Aperture synthesis** – combining multiple baselines
- **(u,v)-plane coverage** increases with more telescopes (baselines), spectral channels, telescope reconfigurations, and with Earth rotation synthesis

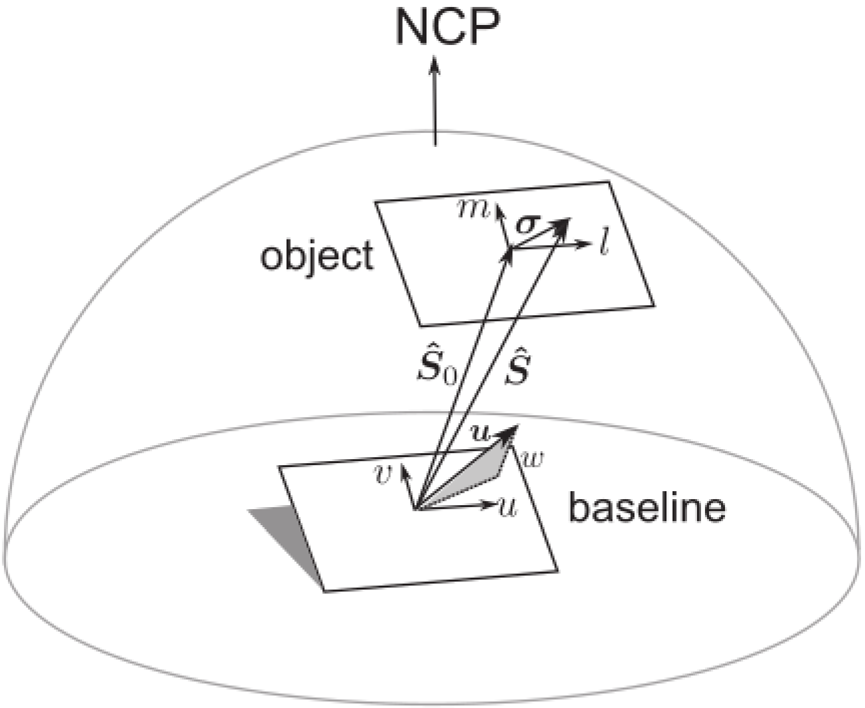

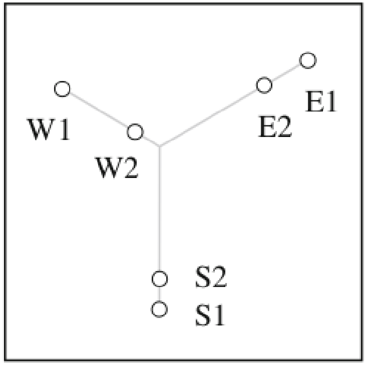

CHARA array

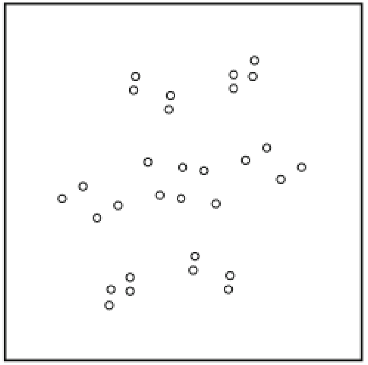
uv-plane

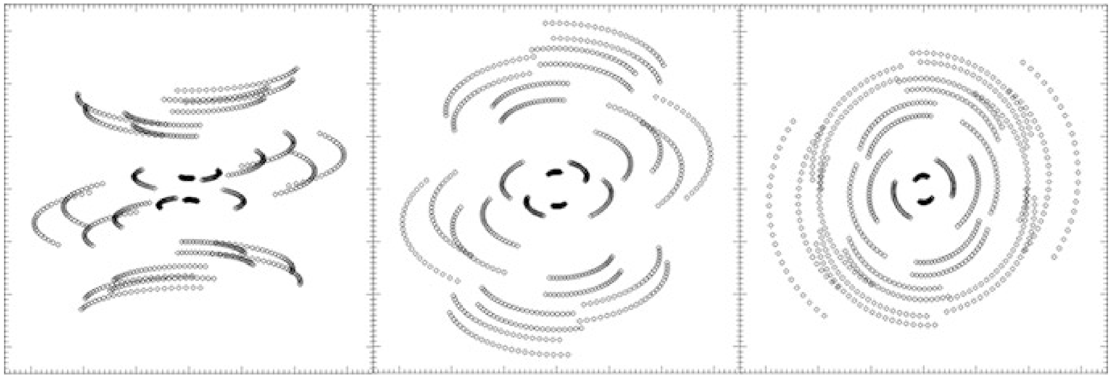

Complex visibility

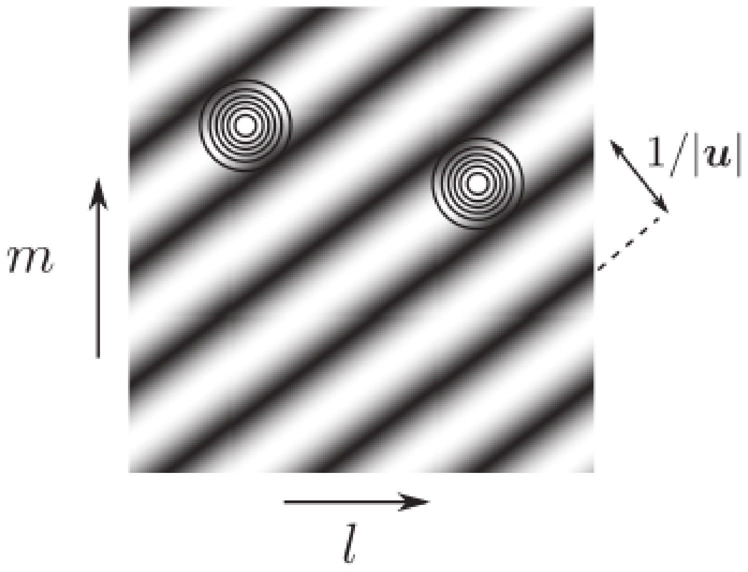

- **Coherent flux** – Flux of the target filtered to pick out structure on the angular scale of the baseline
- Normalized/dimensionless coherent flux is the **complex visibility**
  - Fringe visibility modulus |V|
  - Fringe phase

$$V(\boldsymbol{u}) = \iint_{-\infty}^{\infty} I'(\boldsymbol{\sigma}) e^{-2\pi i \boldsymbol{\sigma}\cdot\boldsymbol{u}}\, dl\, dm$$

Van Cittert-Zernike Theorem - for a monochromatic incoherent source, the Fourier transform of the coherent flux is the angular intensity distribution of the source (*l, m*)

Complex visibility is the Fourier transform of the source

Bandwidth smearing

- Non-zero spectral bandwidth – smearing of fringes offset from phase zero due to non-monochromatic light
- Bandwidth smearing limits the interferometric FoV
- Need large bandwidth to get photons, but need spectral resolution (small bandwidth) to achieve larger FoV

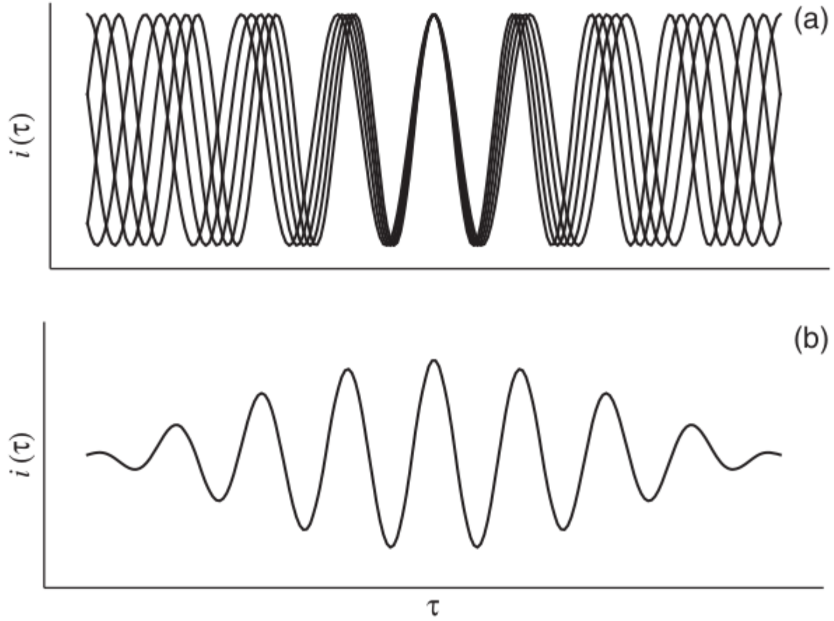

$$\Delta\theta_{\mathrm{FOV}} \sim \Delta\theta_{\mathrm{res}} \frac{\nu_0}{\Delta\nu}.$$

Recording the interference pattern

Pupil-plane beam combination with temporally encoded fringes (CHARA/Classic, CLIMB)

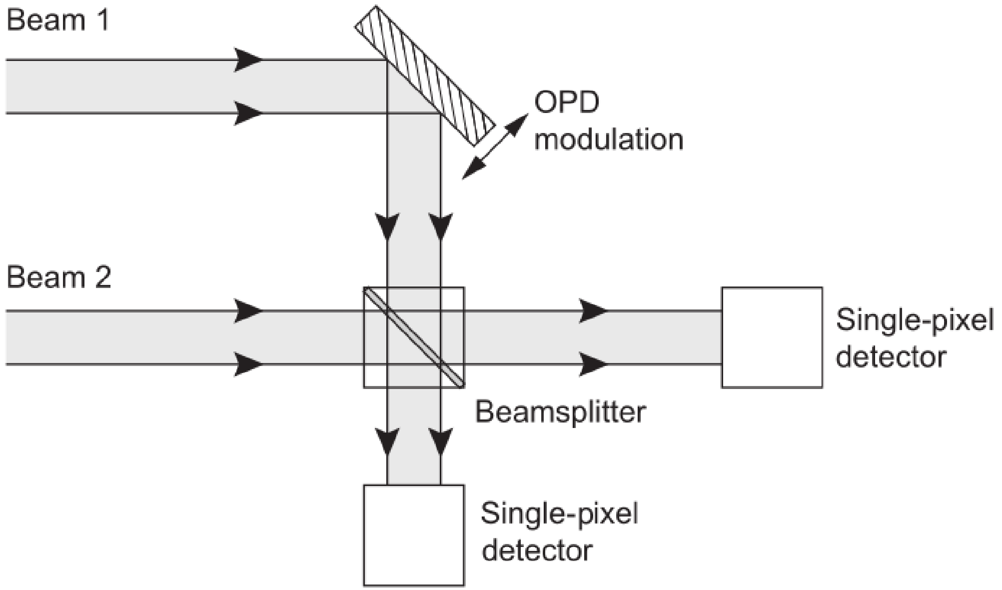

Image-plane beam combination (CHARA/MIRC-X, MYSTIC)

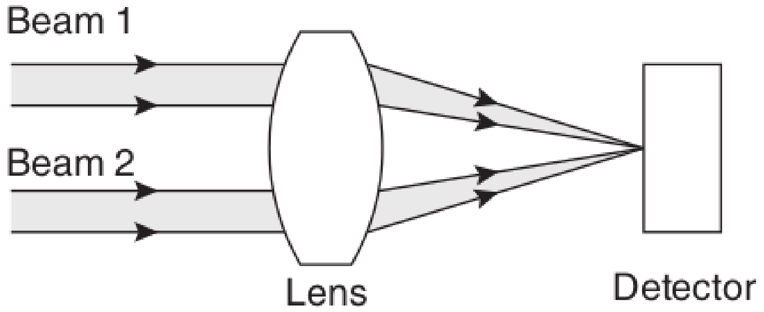

Beam combination for multiple apertures

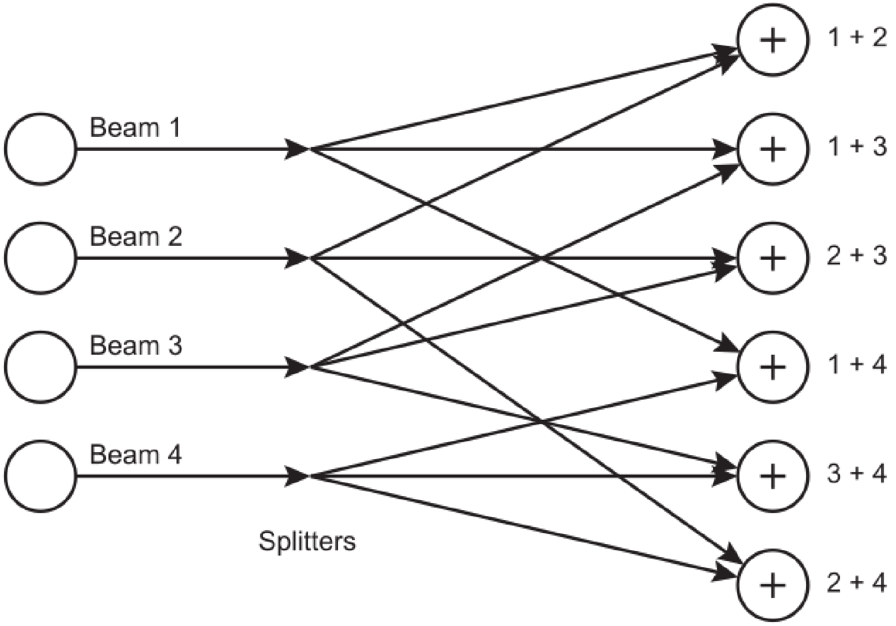

pairwise

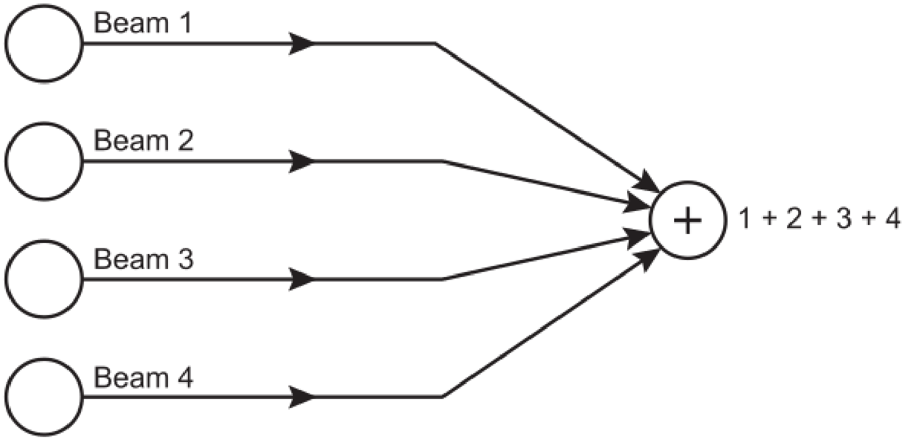

all-in-one redundant configuration

Pairwise combination on an integral optical chip

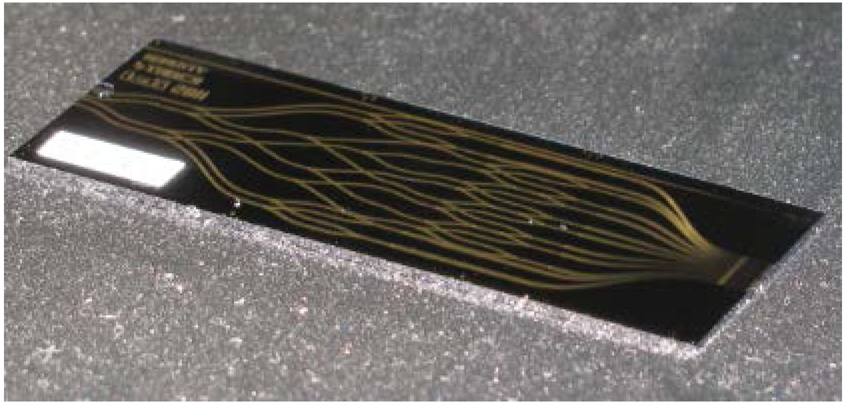

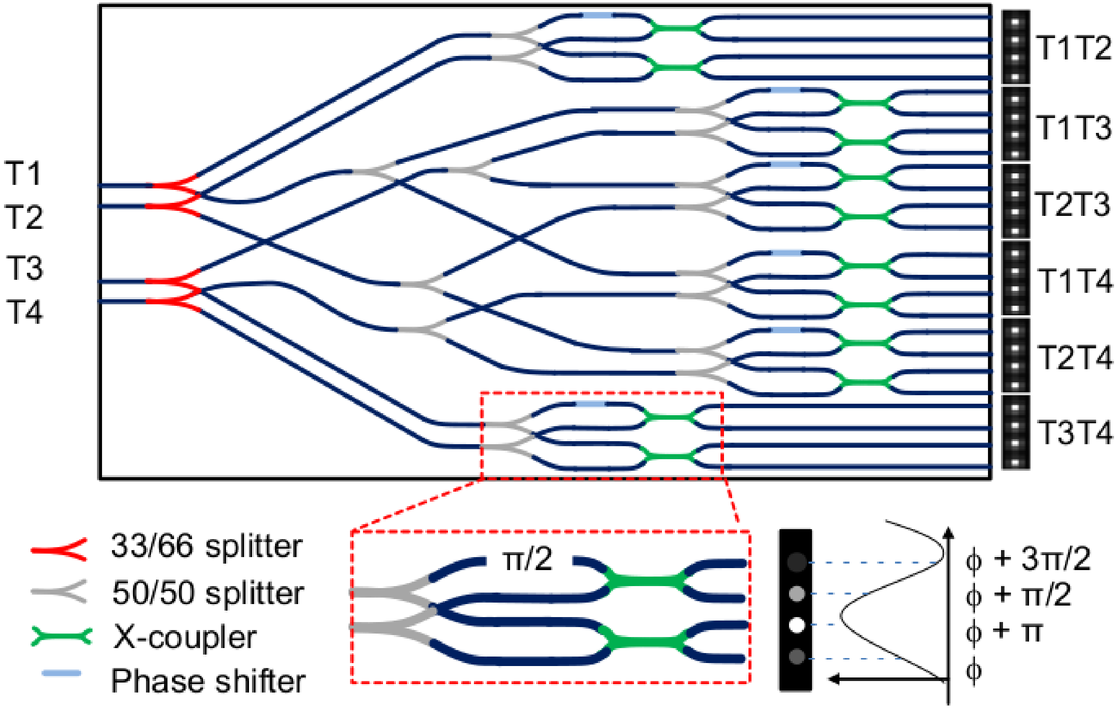

VLTI/PIONIER, VLTI/GRAVITY, CHARA/MYSTIC (special 4T mode for sensitivity)

Measuring complex visibilities in the presence of atmosphere

- Wavefront deformed across the pupils of individual telescopes (when larger than r_0) – decreases fringe contrast – **Spatial Filtering** to sacrifice light outside the first Airy ring (passive AO)
- Atmospheric turbulence introduces phase shifts between individual telescopes (**piston**) which are separated by more than r_0 – compensation by delay lines using **Group Delay and Phase tracking** (Piston AO)

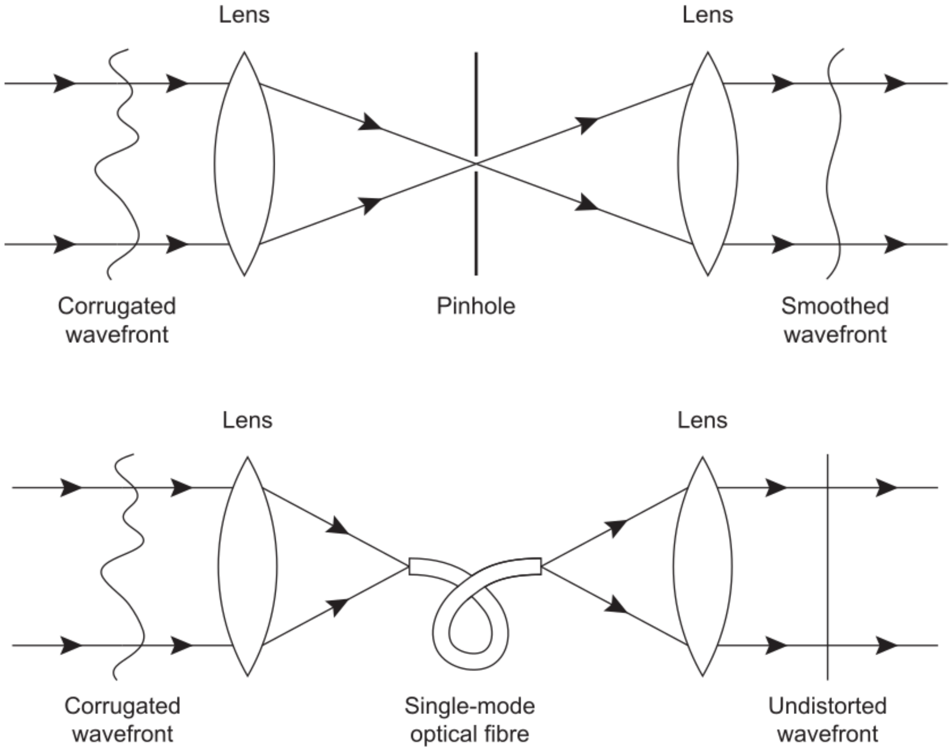

Spatial filtering

Measuring complex visibilities in the presence of atmosphere

- Wavefront deformed across the pupils of individual telescopes (when larger than r_0) – decreases fringe contrast – **Spatial Filtering** to sacrifice light outside the first Airy ring (passive AO)

- Atmospheric turbulence introduces phase shifts between individual telescopes (**piston**) which are separated by more than r_0 – compensation by delay lines using **Group Delay and Phase tracking** (Piston AO)

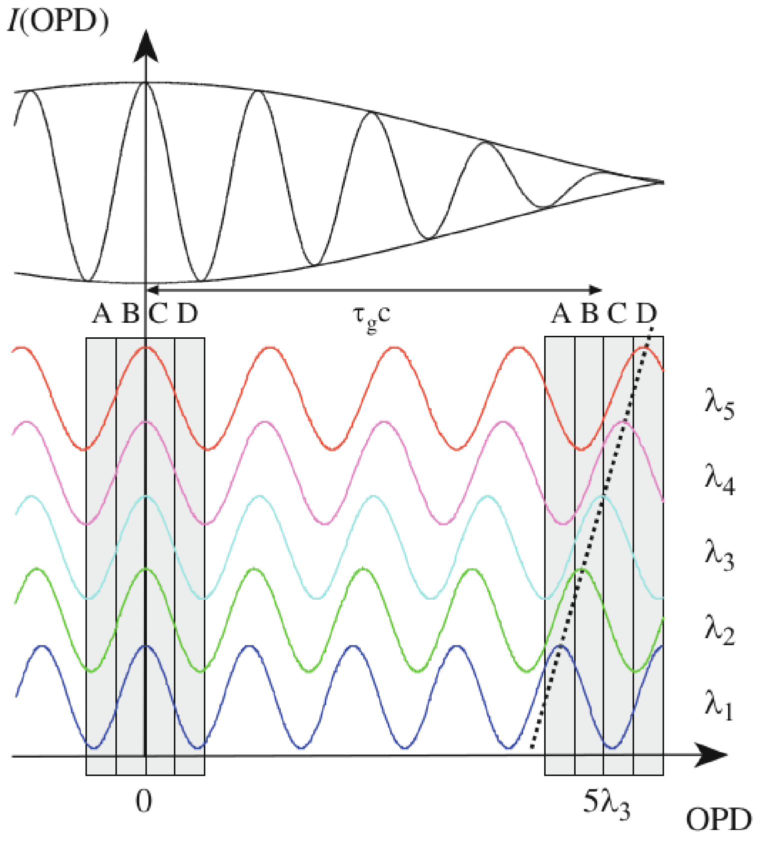

Group delay tracking

Measuring complex visibilities in the presence of atmosphere

- *Phase of the complex visibility for 2-telescope baseline larger than r_0 is lost to the atmosphere*
- **Closure phase** – independent of atmospheric turbulence for a 3-telescope triangle
- **Differential phase** – when investigating spectral lines at high spectral resolution, continuum phase can be normalized to zero

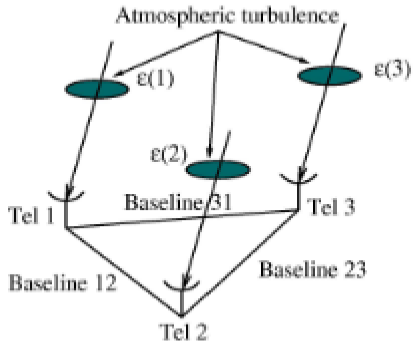

$$\Phi_{pqr} = \Phi_{pq} + \Phi_{qr} + \Phi_{rp}$$

$$\begin{aligned}\Phi_{pqr} &= \phi_{pq} + \epsilon_p - \epsilon_q + \phi_{qr} + \epsilon_q - \epsilon_r + \phi_{rp} + \epsilon_r - \epsilon_p \\ &= \phi_{pq} + \phi_{qr} + \phi_{rp}.\end{aligned}$$

Closure Phase

Measuring complex visibilities in the presence of atmosphere

- Until now we were limited to exposure times < t_0
- **Fringe tracking**
  - AO for interferometry – enables longer exposure times to boost sensitivity
  - employing two beam combiners simultaneously – one to stabilize fringes (low R) and the other to record scientific data (high *R*)

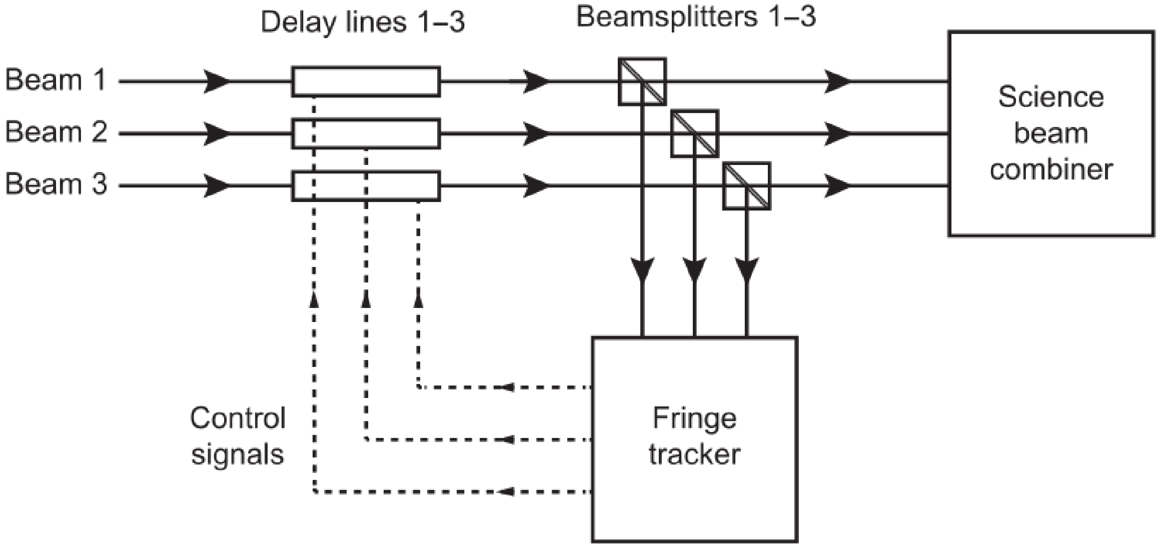

Measuring complex visibilities in the presence of atmosphere

- **Off-axis fringe tracking (dual-field)** capabilities – observing two stars at once, brighter to stabilize fringes

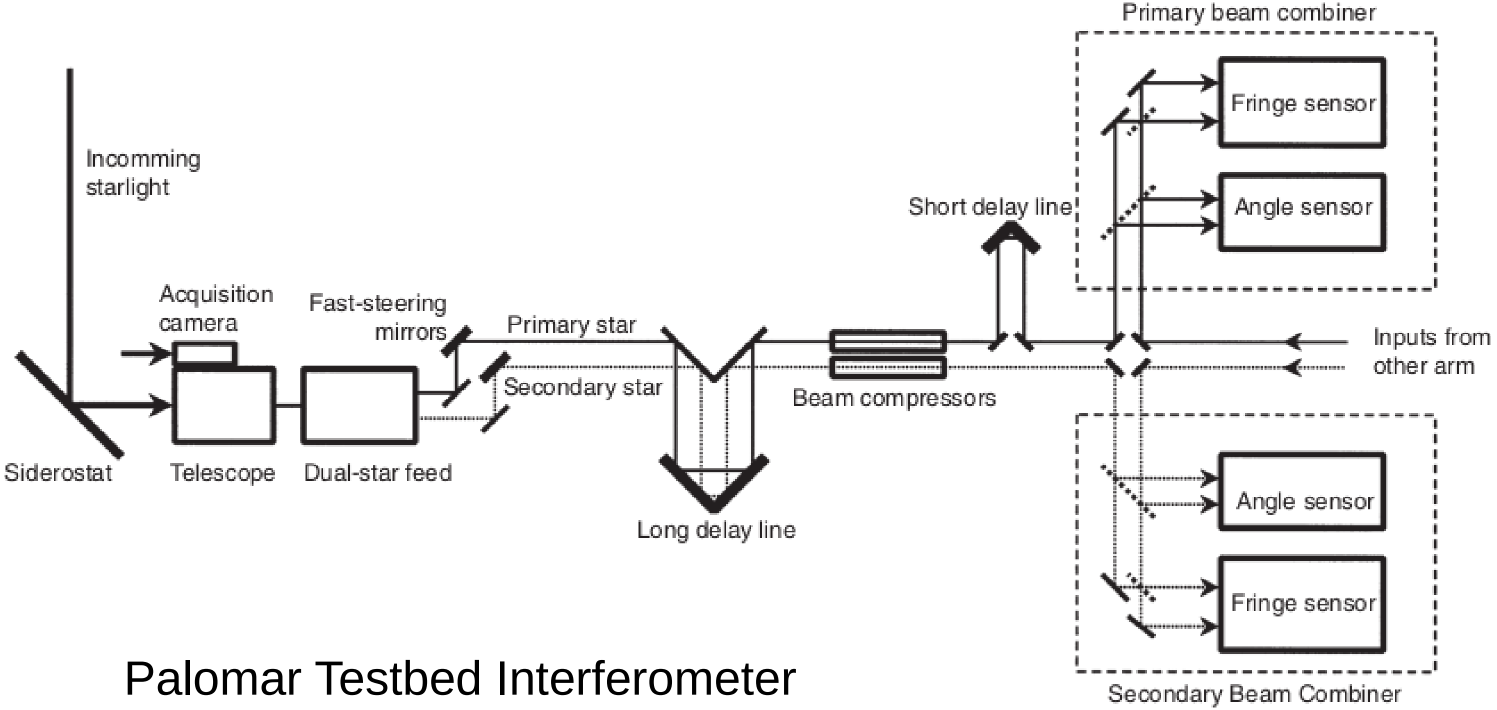

Palomar Testbed Interferometer

Absolute calibration

- Absolute visibility uncertain due atmospheric and instrumental losses – **Transfer Function** needs to be monitored regularly
- Observations of the science target accompanied with observations of calibrators (SCI – CAL concatenations) with small angular diameters (ideally point sources)

Interferometric observables

- 2-telescope baseline
  - Differential and/or absolute Visibility
  - Differential Phase
  - Total number of baselines = (N (N-1)) / 2
- 3-telescope triangle
  - Differential and/or absolute Visibility
  - Differential Phase
  - Closure Phase & Triple amplitude (Phase and amplitude of the bispectrum)
  - Total number of triangles = (N (N-1) (N-2)) / 6

- **Visibility** is sensitive to the size of the object
- **Closure phase** is sensitive to deviations from point symmetry
- **Differential visibility** gives size of the object relative to the size in continuum
- **Differential phase** sensitive to point asymmetry relative to the continuum

Measurement at each baseline *(u,v)* gives a Fourier component of the sky brightness distribution *(l,m)*

Good coverage of (u,v) plane enables modeling and even imaging

Shape	Brightness distribution	Visibility
Point source	$\delta(\vec{x})$	1
Background	I_0	$\begin{cases} 1 & \text{if } \rho = 0 \\ 0 & \text{otherwise} \end{cases}$
Binary star	$I_0\left[\delta(\vec{x}) + R\delta(\vec{x} - \vec{x_0})\right]$	$\sqrt{\frac{1+R^2+2R\cos\left(\frac{\vec{\rho}\cdot\vec{x_0}}{\lambda}\right)}{1+R^2}}$
Gaussian	$I_0\sqrt{\frac{4\ln(2\varnothing)}{\pi}} \times \mathrm{e}^{-4\ln 2\frac{r^2}{\varnothing^2}}$	$\mathrm{e}^{-\frac{(\pi\varnothing\rho)^2}{4\ln 2}}$
Uniform disk	$\begin{cases} \frac{4}{\pi\varnothing^2} & \text{if } r < \frac{\varnothing}{2} \\ 0 & \text{otherwise} \end{cases}$	$\frac{2\mathrm{J}_1(\pi\varnothing\rho)}{\pi\varnothing\rho}$
Ring	$\frac{1}{\pi\varnothing}\delta\left(r - \frac{\varnothing}{2}\right)$	$\mathrm{J}_0(\pi\varnothing\rho)$
Exponential	$\mathrm{e}^{-k_0 r}$, $k_0 \geq 0$	$\frac{k_0^2}{1+k_0^2\rho^2}$
Any circular object	$I(r)$	$2\pi\int_0^\infty I(r)\mathrm{J}_0(2\pi r\rho)rdr$
Pixel (image brick)	$\begin{cases} \frac{1}{lL} & \text{if } x < l \text{ and } y < L \\ 0 & \text{otherwise} \end{cases}$	$\frac{\sin(\pi x l)\sin(\pi y L)}{\pi^2 x y l L}$
Limb-darkened disk	$\begin{cases} I_0[1 - u_\lambda(1-\mu)] & \text{if } r < \frac{\varnothing}{2} \\ \mu = cos(2r/\varnothing) \end{cases}$	$\begin{cases} \frac{\left[\alpha\frac{\mathrm{J}_1(x)}{x} + \beta\sqrt{\pi/2}\frac{\mathrm{J}_{3/2}(x)}{x^{3/2}}\right]^2}{\left(\frac{\alpha}{2}+\frac{\beta}{3}\right)^2} \\ \alpha = 1 - u_\lambda \\ \beta = u_l\lambda \\ x = \pi\theta_{\mathrm{LD}}\frac{B}{\lambda} \end{cases}$

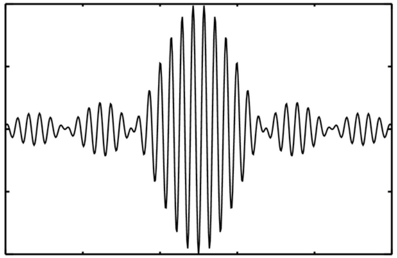

Interferometric observables

Uniform disk

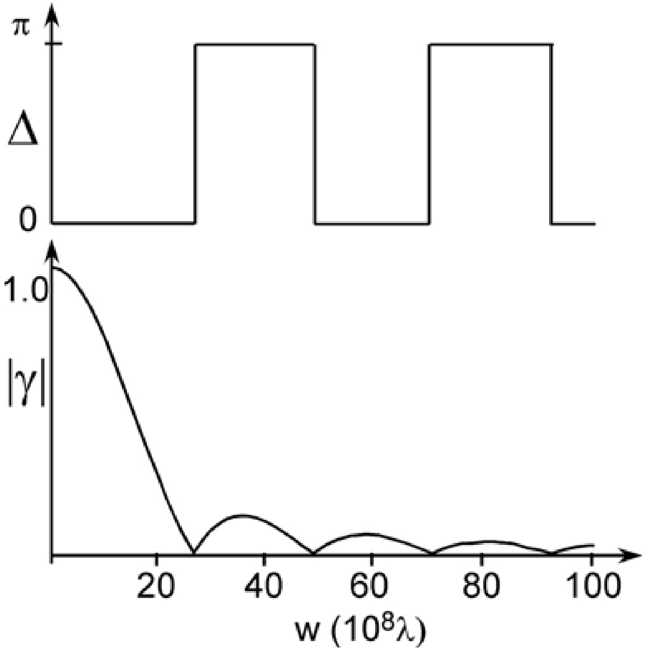

Measuring visibilities for different baselines enables size and shape measurements

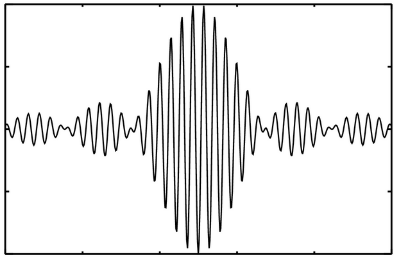

Interferometric observables

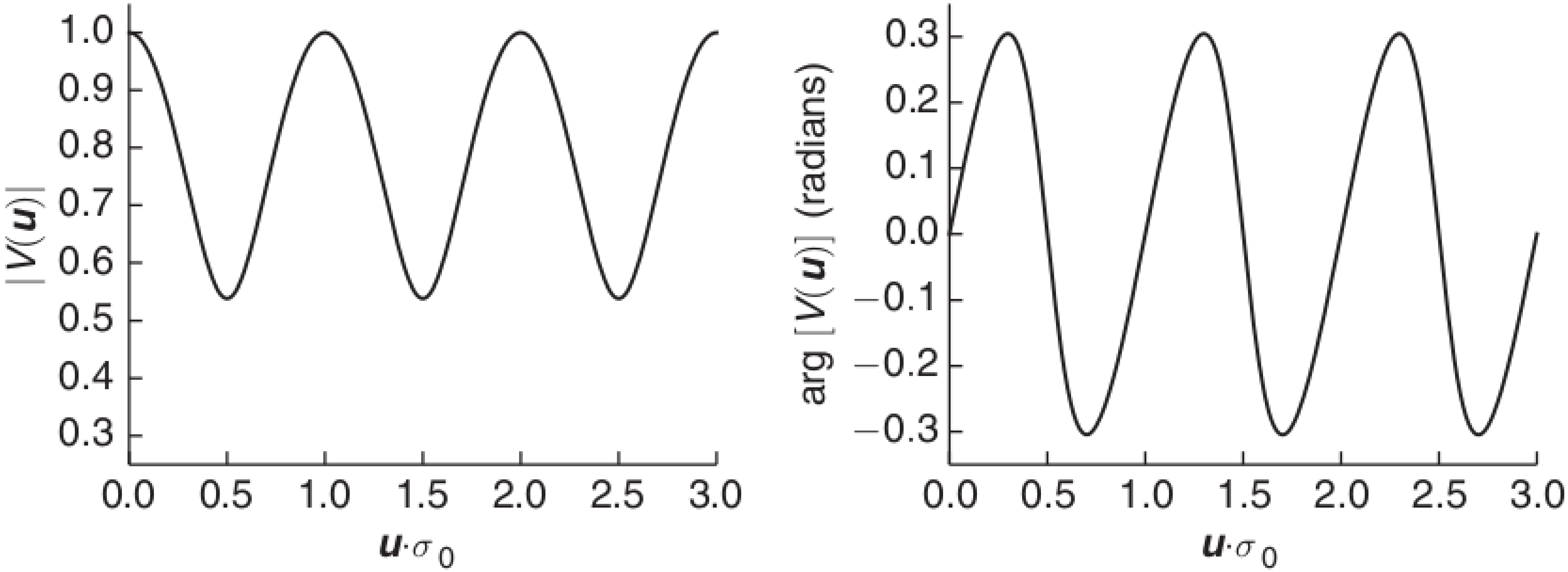

Measuring visibilities for different baselines enables measuring separation and contrast of binaries

Visibility	Closure phase	Diff. Vis.	Diff. Phase
(a) Resolved source Benisty et al. ([2010])	(b) Zero Monnier et al. ([2006])	(c) ↘ in emission line Stee et al. ([2012])	(d) “V” shape Weigelt et al. ([2007])
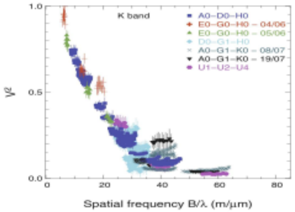	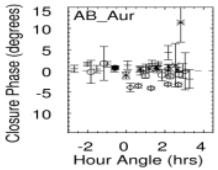	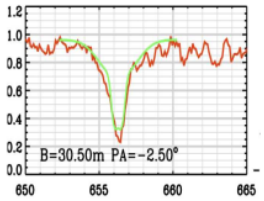	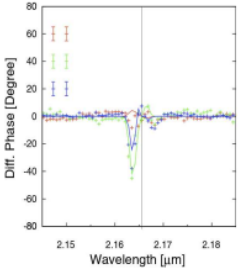
(e) Unresolved source Demory et al. ([2009])	(f) Non-zero Monnier et al. ([2006])	(g) ↗ in emission line Kraus et al. ([2008])	(h) “S” shape Meilland et al. ([2012])
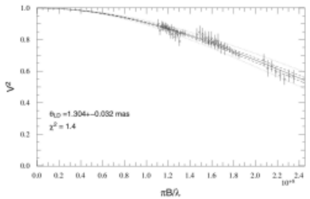	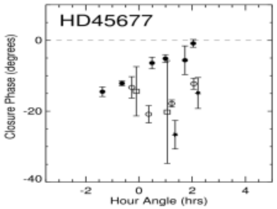	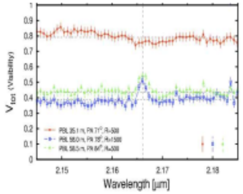	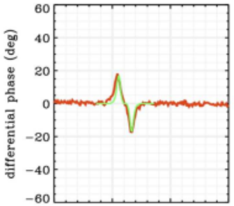
(i) Cosine shape Meilland et al. ([2011])		(j) “W” shape Chesneau et al. ([2011])	(k) Sine shape Meilland et al. ([2011])
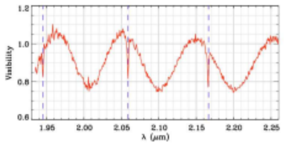		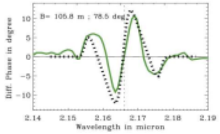	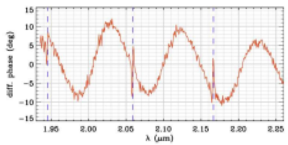

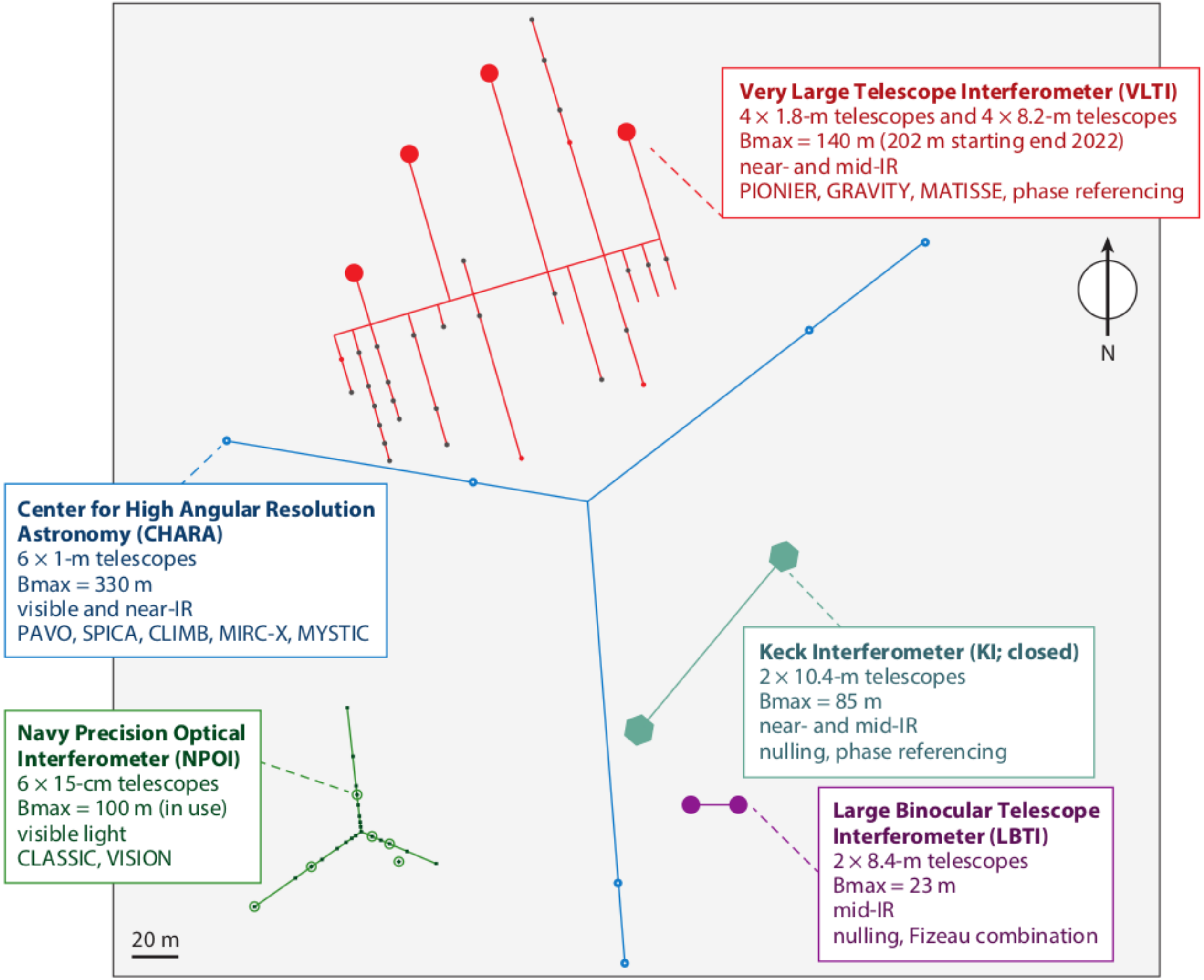

Very Large Telescope Interferometer (VLTI)
4 × 1.8-m telescopes and 4 × 8.2-m telescopes
Bmax = 140 m (202 m starting end 2022)
near- and mid-IR
PIONIER, GRAVITY, MATISSE, phase referencing
N
Center for High Angular Resolution Astronomy (CHARA)
6 × 1-m telescopes
Bmax = 330 m
visible and near-IR
PAVO, SPICA, CLIMB, MIRC-X, MYSTIC
Keck Interferometer (KI; closed)
2 × 10.4-m telescopes
Bmax = 85 m
near- and mid-IR
nulling, phase referencing
Navy Precision Optical Interferometer (NPOI)
6 × 15-cm telescopes
Bmax = 100 m (in use)
visible light
CLASSIC, VISION
Large Binocular Telescope Interferometer (LBTI)
2 × 8.4-m telescopes
Bmax = 23 m
mid-IR
nulling, Fizeau combination
20 m

CHARA Array

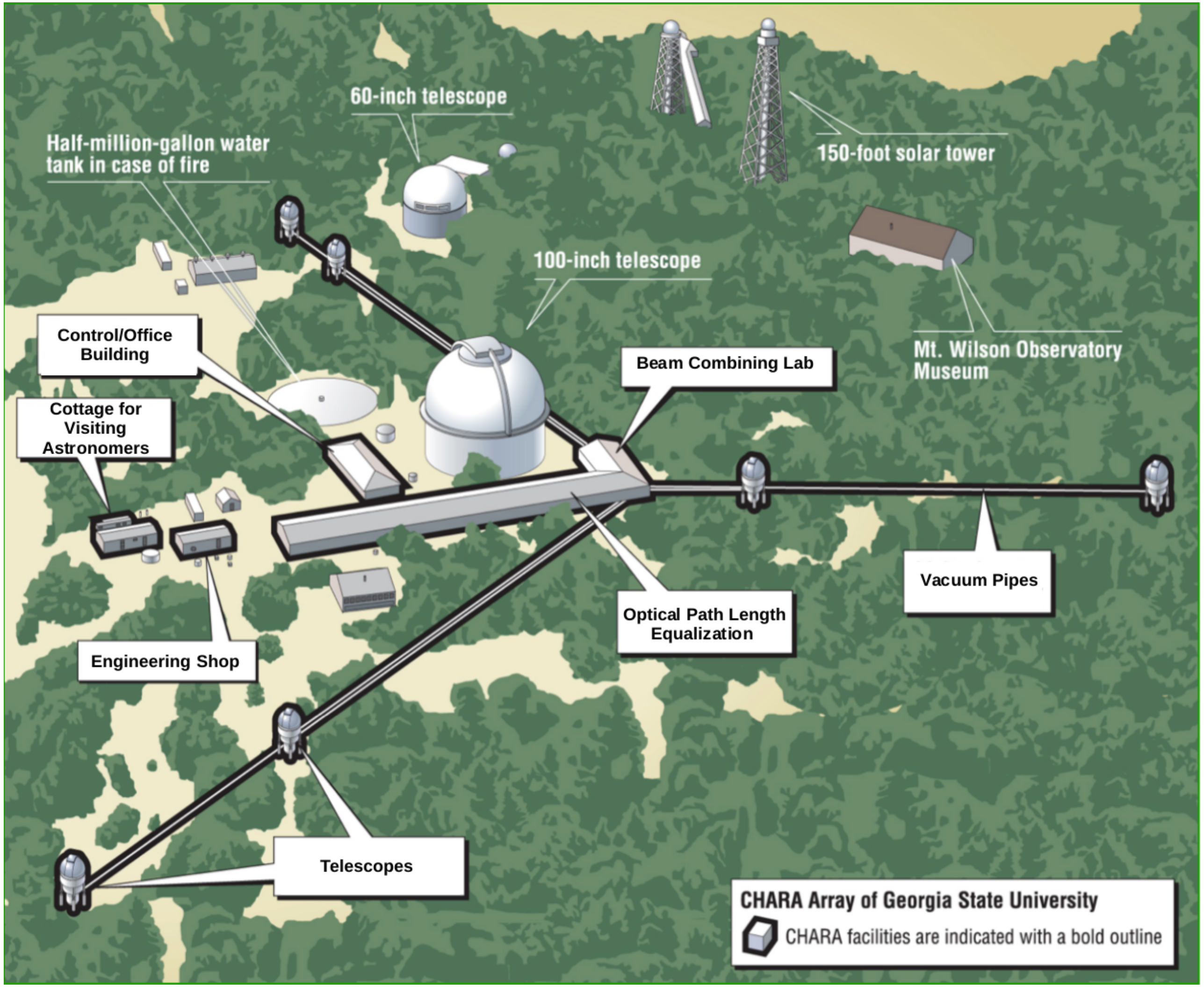

- Six 1-m fixed telescopes with TelAO in Y-shaped configuration
- B_{min} = 33 m; B_{max} = 330 m
- θ ~0.2 mas in *R* to ~0.5 mas in *H*
- Vacuum beam relay pipes & LabAO before optical lab
- Beam combiners
  - Classic/CLIMB – 2T/3T in *K’* band
  - PAVO – 2T in *R* band
  - MIRC-X and MYSTIC – 6T simulteneously in *H* and *K* band
  - SPICA – 6T visible (commissioning)

CHARA Array

- Six 1-m fixed telescopes with TelAO in Y-shaped configuration
- B_{min} = 33 m; B_{max} = 330 m
- θ ~0.2 mas in *R* to ~0.5 mas in *H*
- Vacuum beam relay pipes & LabAO before optical lab
- Beam combiners
  - Classic/CLIMB – 2T/3T in *K'* band
  - PAVO – 2T in *R* band
  - MIRC-X and MYSTIC – 6T simulteneously in *H* and *K* band
  - SPICA – 6T visible (commissioning)

Light collectors / Telescopes

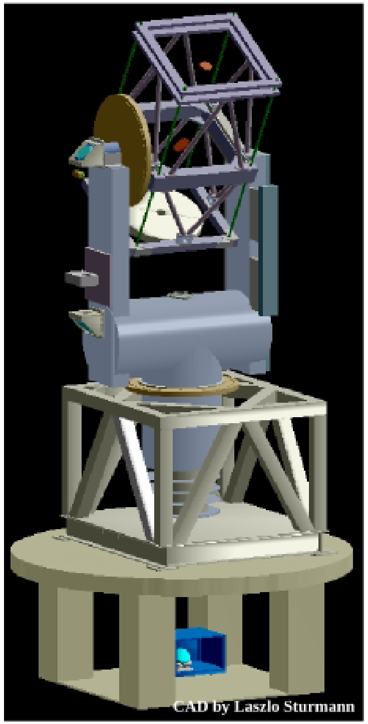

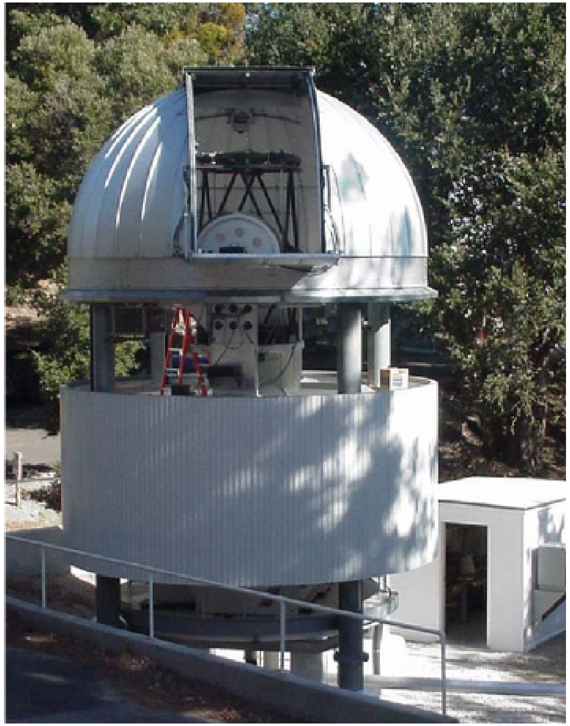

- Collect light and propagate to beam relay
- AO at least on the level of tip-tilt correction
- CHARA has dedicated AO on each telescope

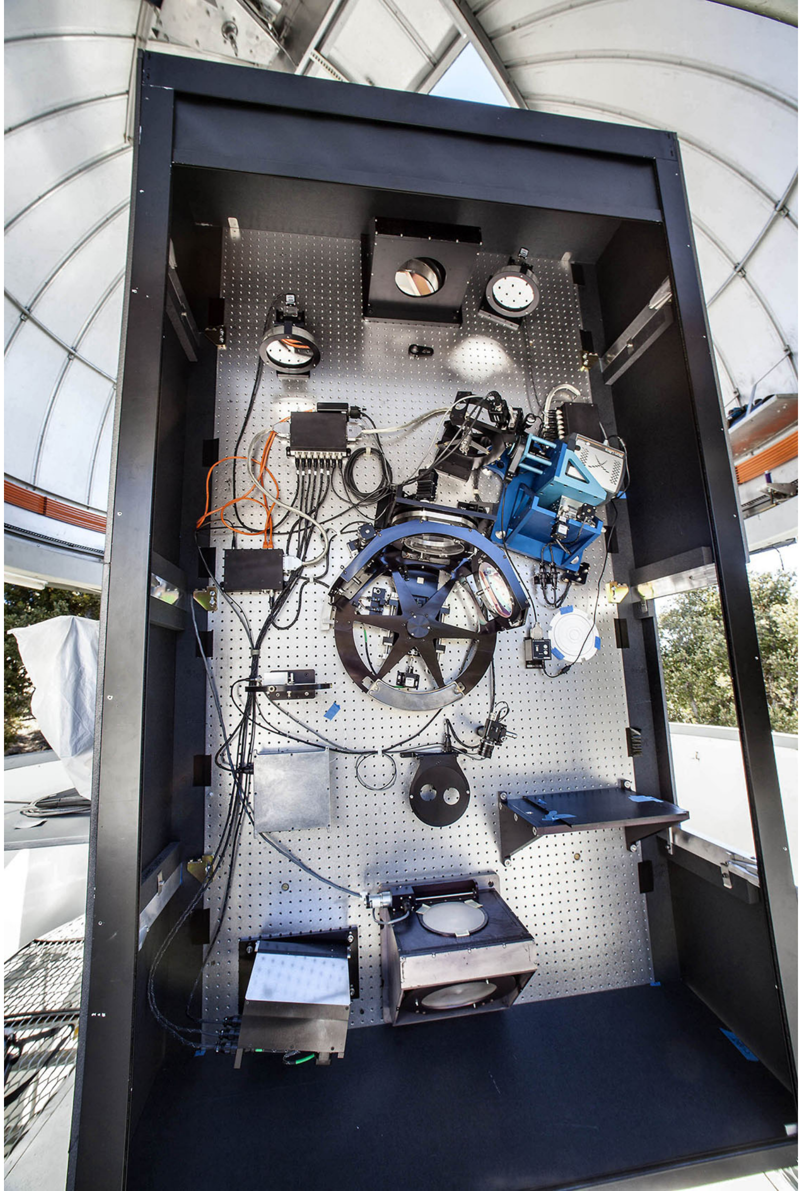

- TelAO on each telescope

Beam relay

- Light propagation from the telescopes to the delay lines and optical lab
- Typically through (vacuum) pipes or tunnels
- Experimental possibilities for the future:
  - Free space propagation
  - Transport through fibers

Delay lines

- Compensate the OPD between the separate beams with a precision of a fraction of the wavelength
- Realized with fine movements of carts on straight rail whose position is measured by Metrology Laser
- Need for elongated spaces to avoid extra reflections

Delay line cart

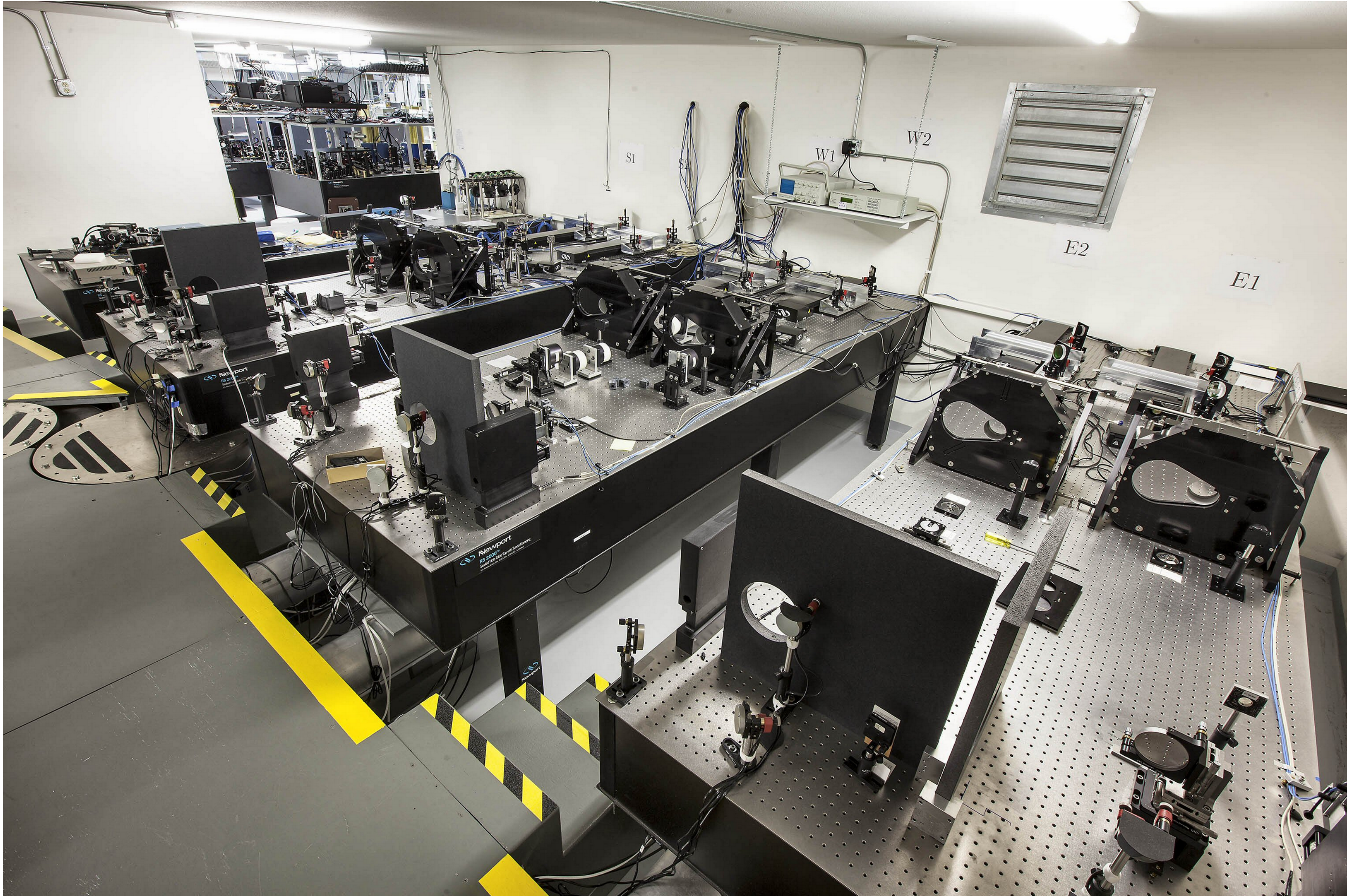
S1
W1
W2
E2
E1
Newport

Optical lab and Beam combination

- Lab AO for each beam
- Different wavelengths can be picked up by different instruments
- CHARA has several different instruments with different characteristics driven by their science goals
- Each instrument has a spectrograph (prism)

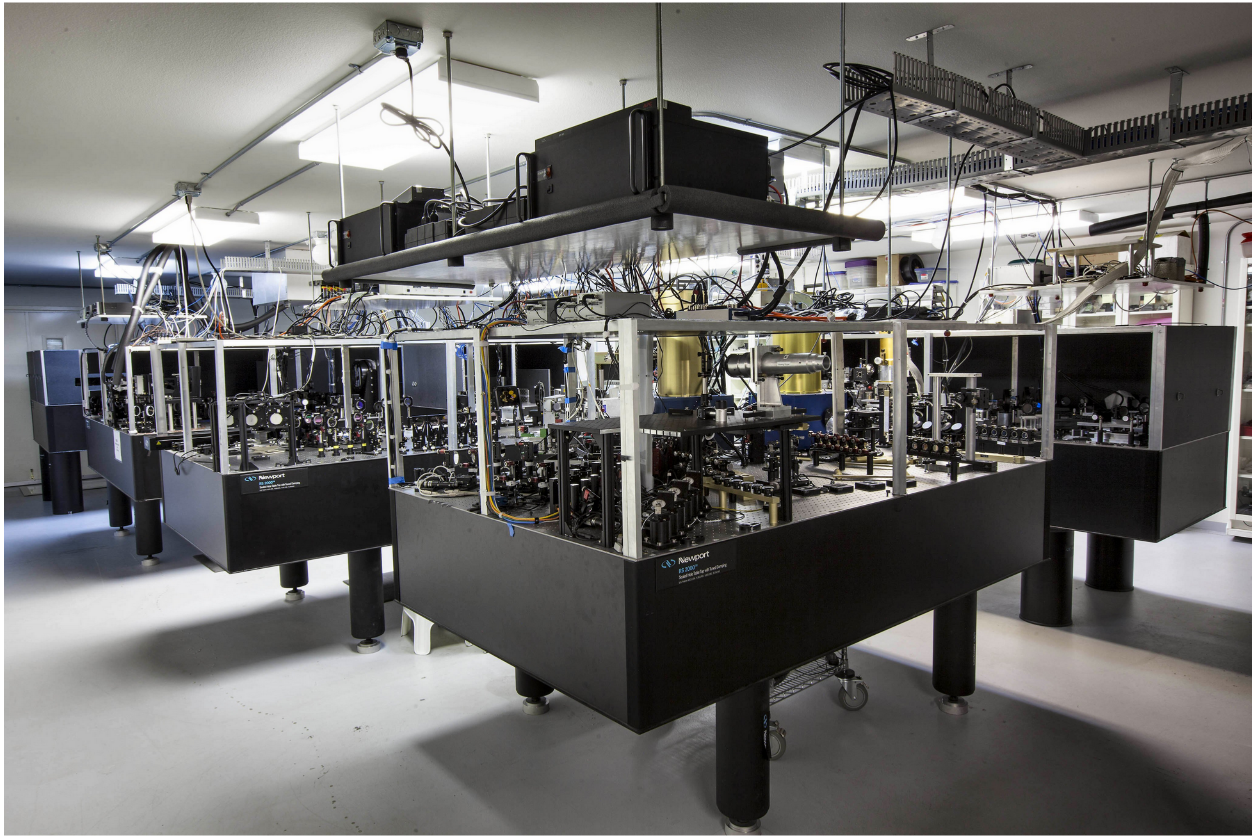

Fringes on MIRC-X and MYSTIC

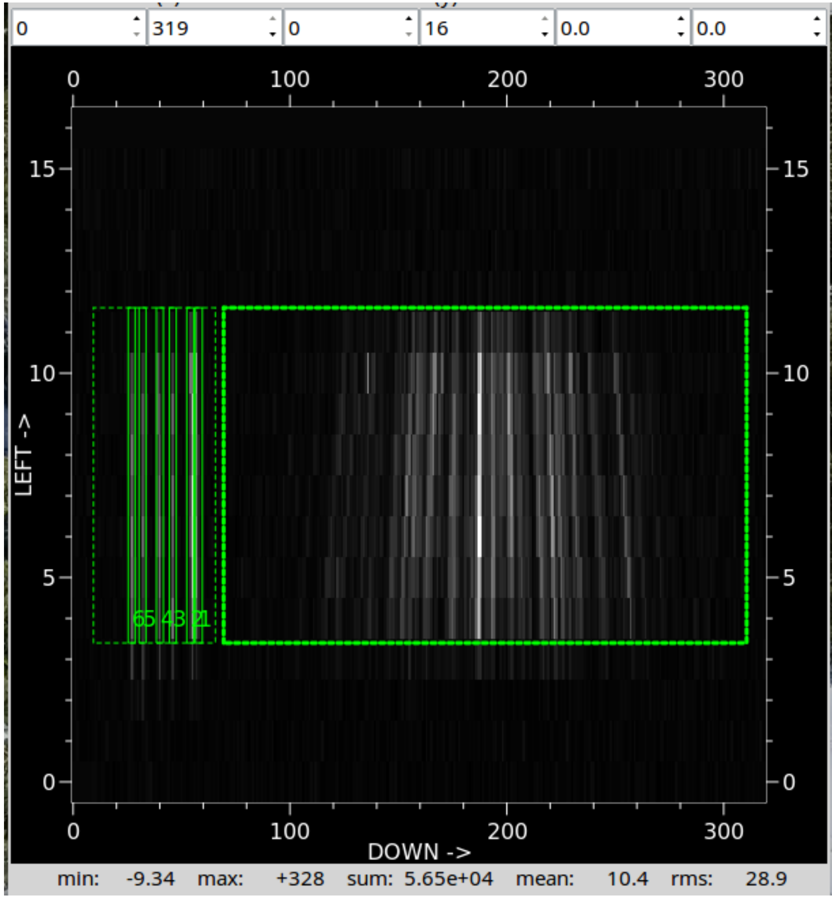

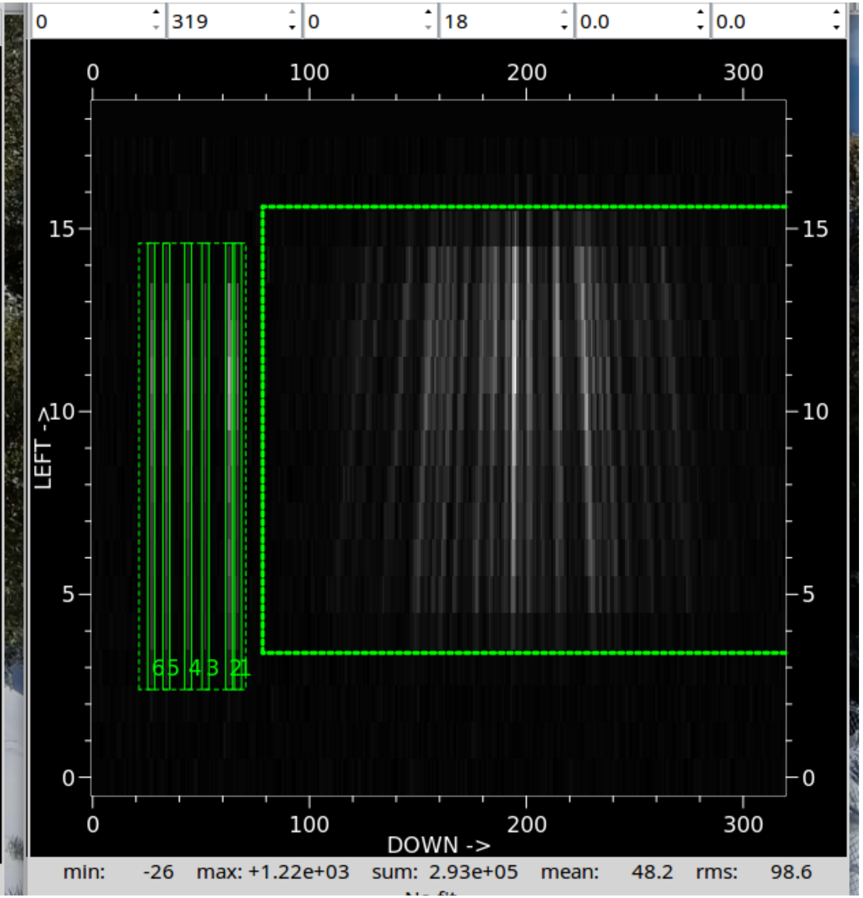

VLTI

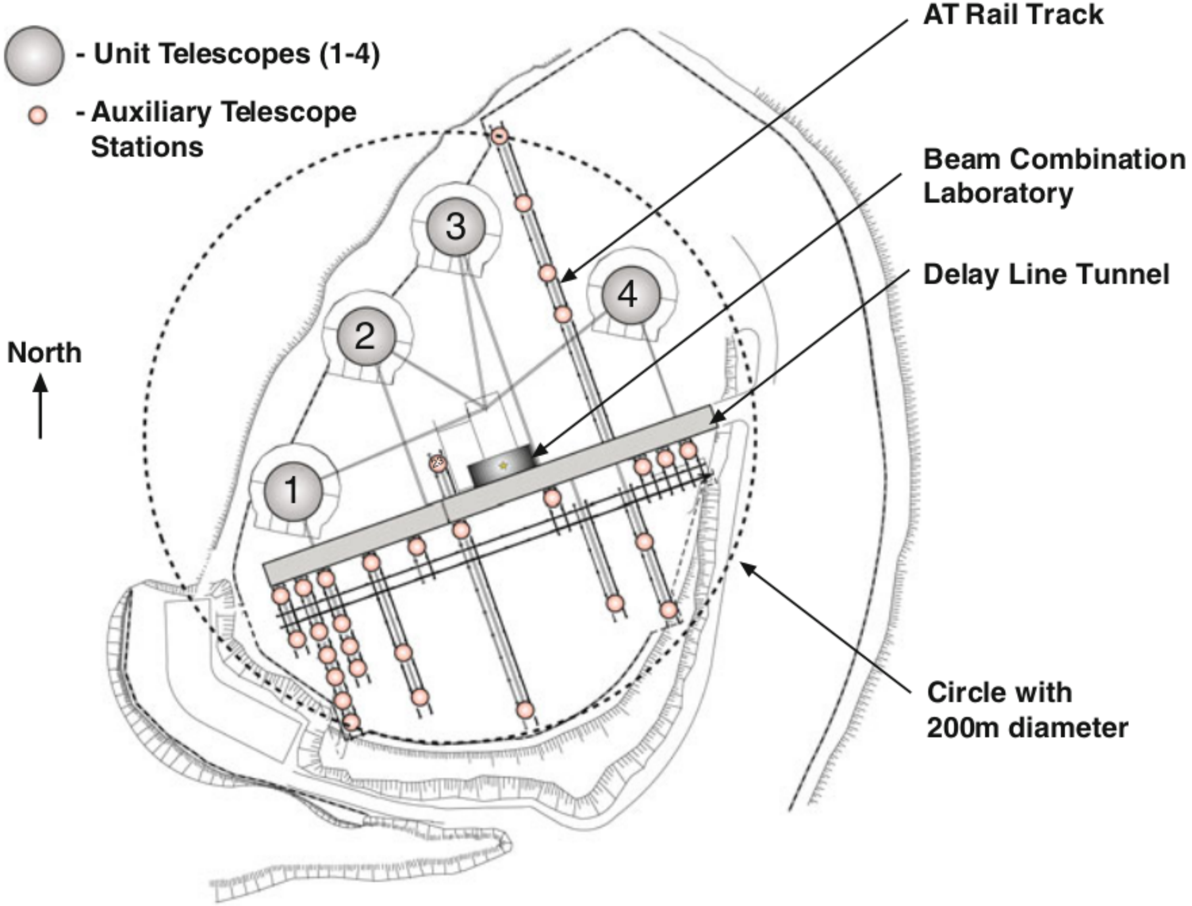

- UT Array and AT Array
- UTs used for VLTI for a ~week each month around full moon
- AT Array configurations
  - Small
  - Medium
  - Large
  - Extended

VLTI

- Four 8-m fixed telescopes or four 1.8-m movable telescopes
- B_{max} ~ 200 m
- θ ~1 mas in *H, K,* ~3 mas in *L*, *M*
- Enables dual-field observations
- Beam combiners
  - PIONIER – 4T in *H* band
  - MATISSE – 4T in *LMN* bands
  - GRAVITY – 4T in *K* band with dual-field mode – great boost in sensitivity
  - GRAVITY+ – Upgrade of observatory infrastructure and UT telescope AO.

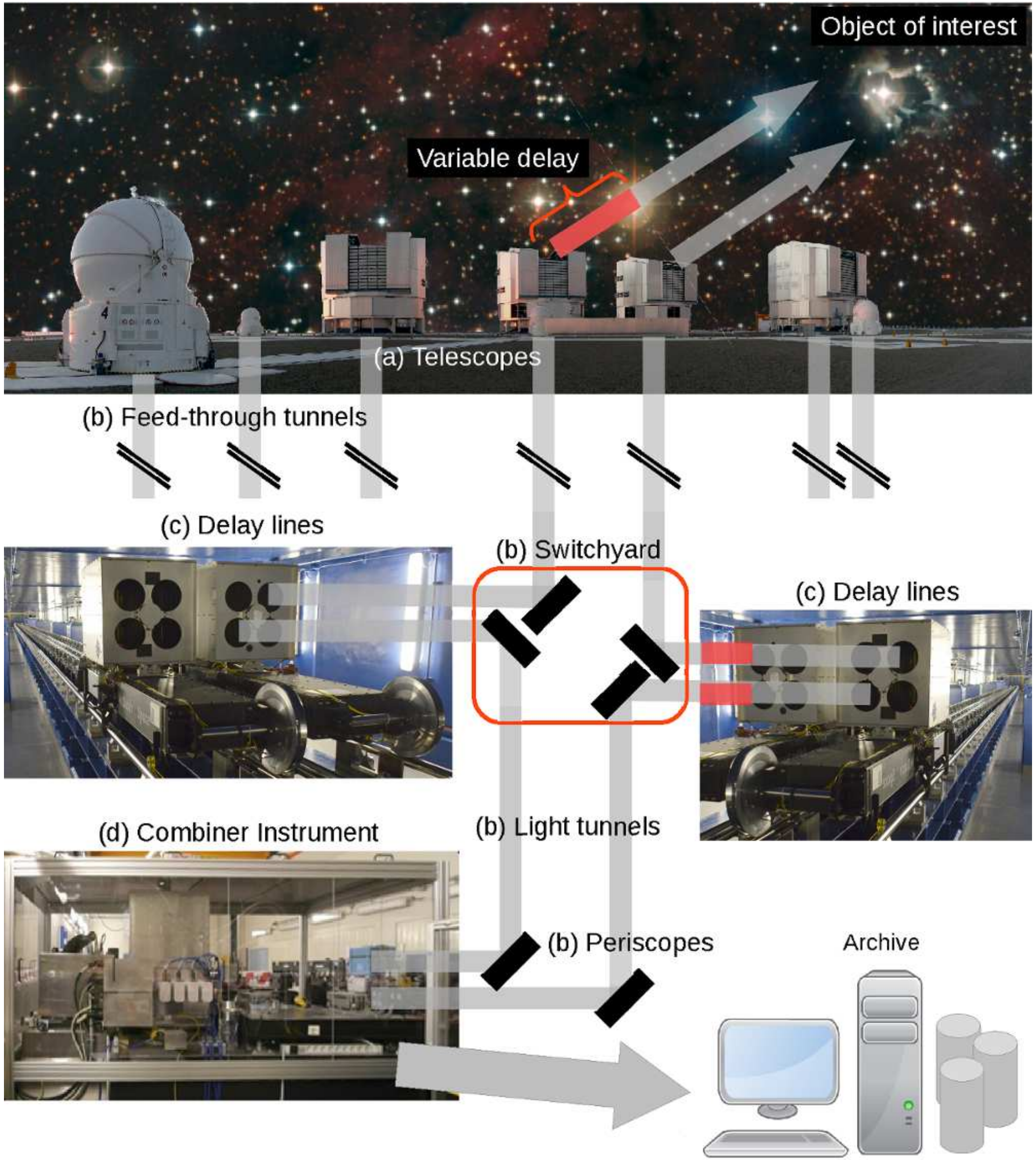

GRAVITY

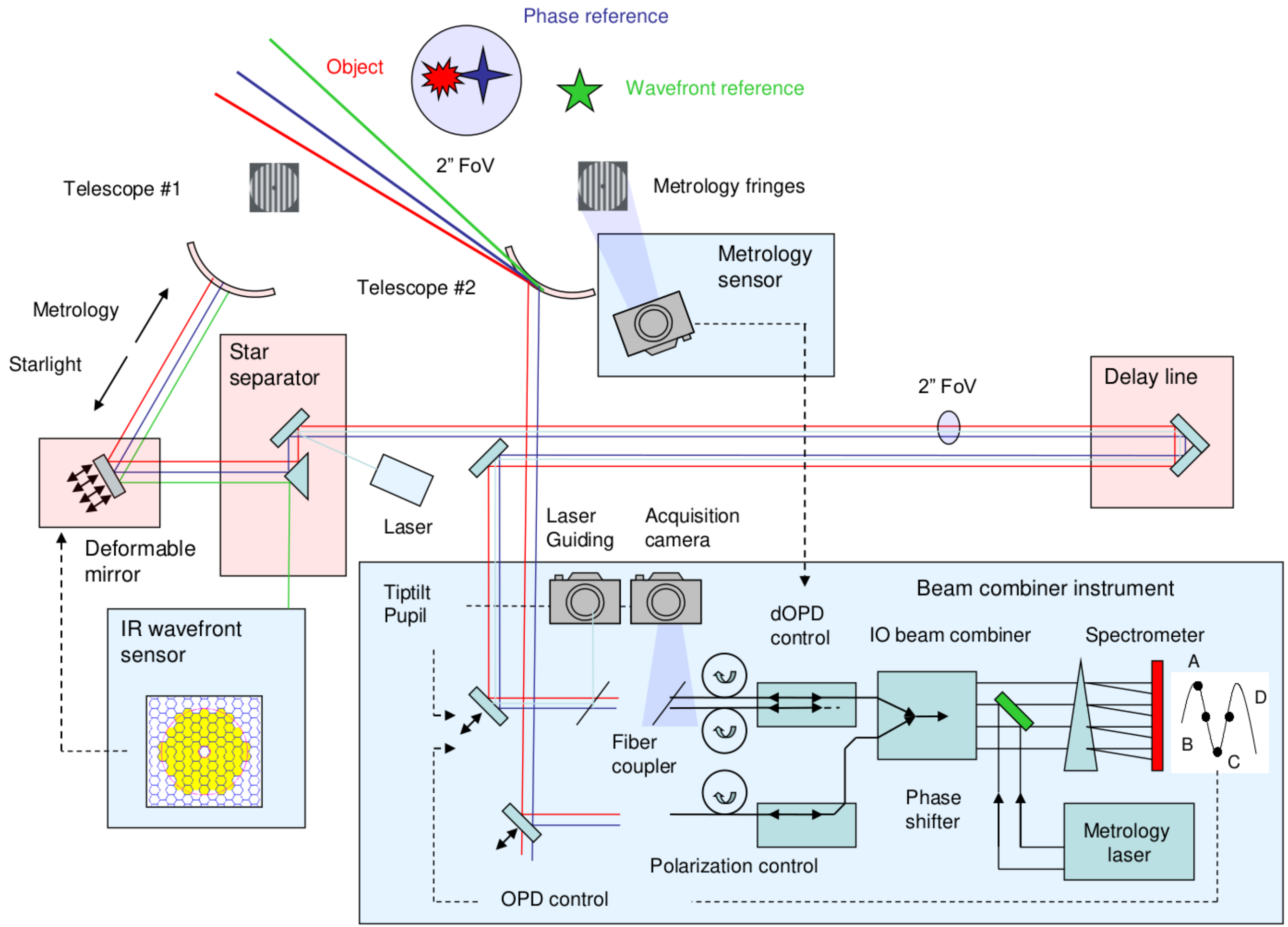

Phase reference
Object
Wavefront reference
2" FoV
Telescope #1
Metrology fringes
Metrology sensor
Telescope #2
Metrology
Starlight
Star separator
2" FoV
Delay line
Laser
Deformable mirror
Laser Guiding
Acquisition camera
Beam combiner instrument
Tiptilt
Pupil
dOPD control
IO beam combiner
Spectrometer
IR wavefront sensor
A
D
B
C
Fiber coupler
Phase shifter
Metrology laser
Polarization control
OPD control

Some take-away messages

- Optical interferometry simulates large telescopes by sacrificing light collection to improve angular resolution – complex systems with many components
- First stellar size measurement >100 years ago, but method maturing only now
- Need to beat atmospheric turbulence with AO and Fringe Tracking to escape the limitation of short exposure times
- CHARA and VLTI are the state-of-the-art arrays currently hosting 2^{nd} generation instruments with more upgrades on the way. MROI under construction.
- Dual-feed beam combiner GRAVITY represents a major boost in sensitivity and is driving the development of new AO system for the UTs at VLT